TECHNICAL UNIVERSITY OF CRETE
SCHOOL OF PRODUCTION
ENGINEERING AND MANAGEMENT

MSc Thesis

# Highway traffic state estimation with mixed connected and conventional vehicles: Microsimulation testing

Markos Fountoulakis
Supervisor: Prof. Markos Papageorgiou

Chania
July 2016

# Thanks

Finalizing this thesis, I would like to thank my supervisor, Prof. Markos Papageorgiou, as well as Prof. Ioannis Papamichail, Dr. Nikolaos Bekiaris-Liberis and Dr. Claudio Roncoli for all their help and guidance during the development of this work.

Most of all, I would like to thank my family for supporting me all these years, as well as my friends and my girl for being there for me.

# Acknowledgement

The research leading to these results has been conducted in the frame of the project TRAMAN21, which has received funding from the European Research Council under the European Union's Seventh Framework Programme (FP/2007-2013)/ERC Advanced Grant Agreement n. 321132.

**Abstract**

This thesis presents a thorough microscopic simulation investigation of a recently proposed methodology for highway traffic estimation with mixed traffic, i.e., traffic comprising both connected and conventional vehicles, which employs only speed measurements stemming from connected vehicles and a limited number (sufficient to guarantee observability) of flow measurements from spot sensors. The estimation scheme is tested using the commercial traffic simulator Aimsun under various penetration rates of connected vehicles, employing a traffic scenario that features congested as well as free-flow conditions. The case of mixed traffic comprising conventional and connected vehicles equipped with adaptive cruise control, which feature a systematically different car-following behavior than regular vehicles, is also considered. In both cases, it is demonstrated that the estimation results are satisfactory, even for low penetration rates.

**Keywords:** traffic estimation, connected vehicles, microscopic simulation

# Contents

# List of Figures

# List of Tables

# Chapter 1

# Introduction

Traffic congestion is a significant problem for the majority of large cities in the modern world (Papageorgiou et al., 2007). While the number of vehicles has been increasing steadily during the past decades (Dargay et al., 2007), a corresponding expansion of road networks is not deemed feasible for various reasons. On the other hand, traffic management represents a valid alternative allowing to improve the performance of traffic systems with fairly moderate effort. For this reason, traffic authorities and automobile industries are currently focusing on the development of innovative methods for traffic monitoring (Bishop, 2005).

Real-time traffic state estimation utilizing limited traffic data is of major importance, not only for traffic monitoring but also for traffic control. In conventional traffic, real-time traffic data are provided by spot sensors positioned at appropriate locations on the highway. Since the cost of installation and maintenance of a sufficient number of spot sensors that guarantees accurate traffic monitoring is high, several studies deal with the development of traffic estimation algorithms employing a limited amount of sensors, such as, for example, Muñoz et al. (2003), Alvarez-Icaza et al. (2004), Wang and Papageorgiou (2005), Hegyi et al. (2006), Mihaylova et al. (2007), Morbidi et al. (2014), to name only a few.

The eminent need for improvement of traffic conditions, for enhancement of driver safety and comfort, and for reduced operation cost of traffic systems has led to the introduction of various Vehicle Automation and Communication Systems (VACS). VACS capabilities can be exploited for the development of novel traffic estimation and control methodologies (Diakaki et al., 2015). Traffic control in the presence of VACS is the subject of numerous papers, such as, for example, Varaiya (1993), Rao and Varaiya (1994), Rajamani and Shladover (2001), Bose and Ioannou (2003), Kesting et al. (2008), Shladover et al. (2012), Ge and Orosz (2014), Wang et al. (2014), Roncoli et al. (2015), Roncoli et al. (2016).

The problem of traffic estimation in the presence of VACS is addressed in numerous studies, such as, for example, Work et al. (2008), De Fabritiis et al. (2008), Herrera et al. (2010), Rahmani et al. (2010), Treiber et al. (2011), Gayah and Dixit (2013), Yuan et al. (2012), Ramezani and Geroliminis (2012), Piccoli et al. (2015), Seo et al. (2015), Bekiaris-Liberis et al. (2016), Roncoli et al. (2016) to name only a few. Typically, such traffic state estimation algorithms employ data stemming from connected vehicles, i.e., vehicles that can provide real-time information to a central or local authority (Turksma, 2000). Connected vehicle data can be utilized as a low-cost and efficient, complementary or primary, source of traffic information towards traffic state estimation (Treiber and Kesting, 2013).

In addition to vehicle communication systems, automated vehicle systems play an important role in modern intelligent transportation systems. While fully automated highways, an innovation that would affect traffic conditions significantly (Kesting et al., 2007), are unlikely to come into existence in the near future, partially automated highways are already part of reality. One of the crucial components of such automated systems is Adaptive Cruise Control (ACC), which was already introduced into modern vehicles by the automobile industry (Darbha and Rajagopal, 1999; Wang et al., 2014). ACC-equipped vehicles aim at increased driver safety and improved comfort (Dragutinovic et al., 2005) and may have a different car-following behavior than manually driven cars, thus changing the traffic flow characteristics accordingly. Since a high penetration rate of ACC-equipped vehicles is not yet a reality, the effect of various percentages of such vehicles on traffic conditions is typically examined utilizing microscopic simulation platforms, see, e.g., Treiber and Helbing (2001), Marsden et al. (2001), VanderWerf et al. (2001), Rajamani et al. (2005), van Arem et al. (2006), Kesting et al. (2007), Ntousakis et al. (2015).

In this text, the research on the validation of the scheme developed in Bekiaris-Liberis et al. (2016) for estimation of densities and ramp flows, which is based on a simple but exact macroscopic model for traffic density and employs mainly speed measurements obtained from connected vehicles (equipped with ACC or not), is continued and extended. The distinguishing characteristic of this estimation scheme, compared to virtually all previous related developments, is that it is only based on the conservation-of-vehicles equation, without the resort of fundamental diagrams or other empirical relationships, which would call for appropriate and tedious model validation procedures, before field application. The performance of the estimation scheme is tested under mixed traffic conditions, where connected vehicles, equipped with ACC or not, are present at various penetration rates. The microscopic simulation software Aimsun (Transport Simulation Systems, 2014) is utilized for the

testing, in which a highway stretch that includes several on-ramps and off-ramps is built, and a scenario in which both congested and free-flow traffic conditions occur is employed. Moreover, the performance of the estimation scheme is evaluated when, for some instances, a very limited (or literally zero) number of speed measurements from connected vehicles are available, and simple algorithms for resolving the problem of lack of reliable segment speed measurements are proposed. Additionally, it is demonstrated that density estimation is highly insensitive to the choice of the filter parameters, while ramp flow estimation is more sensitive.

# Chapter 2

# Traffic state estimation exploiting VACS capabilities

## 2.1 Innovative features of VACS

### 2.1.1 Connected vehicles

Data stemming from connected vehicles may contain a wide variety of traffic information, but the most commonly used are vehicle position (longitude, latitude, and altitude) and vehicle speed. The most popular way of acquiring a vehicle's position is via the Global Positioning Systems (GPS), see, e.g., De Fabritiis et al. (2008), Rahmani et al. (2010), Herrera et al. (2010), although cellular positioning is also utilized, usually with less accurate results, see, e.g., Yim and Cayford (2001), Bar-Gera (2007). GPS is a low-cost, efficient solution to gather traffic data, with a reported position error of 5–15 m in older studies (Zito et al., 1995; Turksma, 2000), whereas recently, with the employment of Differential GPS (DGPS) and map-matching algorithms, position accuracy up to 1–5 m can be achieved (Waterson and Box, 2012). Speed measurement error is mostly reported to be as low as 1 km/h (Zito et al., 1995), reaching 5 km/h in some studies (Zhao et al., 2011). Data from connected vehicles are mainly transmitted to a central traffic authority, which reflects the so called Vehicle to Infrastructure (V2I) communication, typically via a GPRS/GSM network (Bishop, 2005). In parallel, vehicles can send data to one another, via Vehicle to Vehicle (V2V) communication, usually utilizing WiFi 802.11 (Waterson and Box, 2012). Connected vehicle data are usually small in size, thus low-delay transmissions are possible (Messelodi et al., 2009). Reporting periods vary among different experiments and commercial systems, most frequently ranging between a few seconds and a few minutes, see, e.g., Bishop (2005), Zhang et al.

(2007), Messelodi et al. (2009), Herrera et al. (2010).

### 2.1.2 Automated vehicles

As part of the Advanced Driver Assistance Systems (ADAS), earlier cruise control systems were designed to merely maintain a certain speed set by the driver. However, novel ACC systems are able, additionally to the cruise control feature, to preserve a predefined safety time-gap to the leading vehicle (Bishop, 2005). Usually, the desired ACC time-gap ranges between 0.9 and 2.5 s (Kesting et al., 2007), but might go as low as 0.5 s (van Arem et al., 2006). The objective of the ACC system is to compute and apply the appropriate acceleration or deceleration according to the driver settings and the surrounding conditions. In order for this to happen, information about the vehicle ahead is required, more specifically, the distance (space gap) and speed difference of the two vehicles, which can be obtained via on-board sensors (Kesting et al., 2007). Using this information, the ACC system calculates the necessary acceleration or deceleration and transforms it to actual throttling or breaking commands. Since the ACC system acquires knowledge of the preceding vehicle's position and speed (e.g., by measuring via on-board sensors the spacing and relative speed with respect to the preceding vehicle as well as its own position and speed), this information could be used to enhance the traffic information reported by an ACC-equipped connected vehicle, thus providing two speed measurements to the central authority instead of one. For more information on available ACC models and technologies, see, e.g., Bishop (2005), Rajamani et al. (2005), Diakaki et al. (2015), Ntousakis et al. (2015).

## 2.2 Traffic estimation using average speed measurements

### 2.2.1 Traffic density dynamics as an LPV system

The density $\rho_i(k)$ of highway segment $i$ at time step $k$ is considered to be the number of vehicles at the segment divided by the segment length $\Delta_i$. The dynamics of the density can be described by the following discrete-time equations

$$\rho_i(k+1) = \rho_i(k) + \frac{T}{\Delta_i}\left(q_{i-1}(k) - q_i(k) + r_i(k) - s_i(k)\right), \tag{2.1}$$

where $i = 1, \ldots, N$ is the index of the specific highway segment of the network, $k$ is the discrete time index, $\Delta_i$ is the length of segment $i$ (km), $q_i$ is the flow (veh/h)

at the end of segment $i$ and $T$ is the time-discretization step (h); $r_i$ and $s_i$ are the vehicle inflow and outflow (veh/h) of on-ramps and off-ramps at the specific segment, respectively. Typically, a highway segment contains only one on-ramp or one off-ramp. Given that

$$q_i(k) = \rho_i(k)\upsilon_i(k), \tag{2.2}$$

where $\upsilon_i(k)$ is the average vehicle speed of segment $i$ at time $k$, (2.1) can be rewritten as

$$\rho_i(k+1) = \frac{T}{\Delta_i}\upsilon_{i-1}(k)\rho_{i-1}(k) + \left(1 - \frac{T}{\Delta_i}\upsilon_i(k)\right)\rho_i(k) + \frac{T}{\Delta_i}\left(r_i(k) - s_i(k)\right). \tag{2.3}$$

In order for the discrete-time relations described by (2.1) and (2.2) to be sufficiently accurate, the following inequality must hold

$$\max_{i,k} \frac{T}{\Delta_i} v_i(k) < 1. \tag{2.4}$$

Assuming that the average speed of vehicles at a segment, namely $v_i$, is measured (e.g. from connected vehicle reports) the state

$$x = (\rho_1, \ldots, \rho_N)^T \tag{2.5}$$

is defined. The deterministic part of the dynamics of segment densities given in (2.3) can be written in the form of a Linear Parameter-Varying (LPV) system as

$$x(k+1) = A(k)x(k) + Bu(k), \tag{2.6}$$

where

$$A(k) = \begin{cases} a_{ij} = \frac{T}{\Delta_i} v_{i-1}(k), & \text{if } i - j = 1 \text{ and } i \geq 2 \\ a_{ij} = 1 - \frac{T}{\Delta_i} v_i(k), & \text{if } i = j \\ a_{ij} = 0, & \text{otherwise} \end{cases} \tag{2.7}$$

$$B = \begin{cases} b_{ij} = \frac{T}{\Delta_i}, & \text{if } i = 1 \text{ and } j = 1 \\ b_{ij} = 0, & \text{otherwise} \end{cases} \tag{2.8}$$

$$u(k) = \left[\, q_0(k)\ r_1(k) - s_1(k)\ \ldots\ r_N(k) - s_N(k) \,\right]^T \tag{2.9}$$

$$C = \left[\, 0\ \ldots\ 0\ 1 \,\right] \tag{2.10}$$

with $A \in \mathbb{R}^{N \times N}$, $B \in \mathbb{R}^{N \times (N+1)}$. Note that $q_0$, which is assumed to be measured (for example, via fixed flow detector), is the flow of vehicles at the entry of the considered highway stretch and acts as an input to (2.6); along with on-ramp and off-ramp flows, $r_i$ and $s_i$, respectively; while $v_i$, $i = 1, \ldots, N$, are viewed as time-varying parameters of (2.6). LPV systems are a well-studied subclass of linear time-varying systems, whose dynamics vary as a result of the variation of certain parameters.

Regarding the output, the density (or equivalently, the flow) at the mainstream exit of the highway is assumed to be available and can be computed via a fixed flow detector as

$$\rho_N = \frac{q_N}{v_N}, \tag{2.11}$$

where $v_N$ is the speed of the last segment as reported by connected vehicles.

Although it is physically intuitive that the system described in (2.6)–(2.10) is observable, the detailed proof that the system is indeed observable can be found in Bekiaris-Liberis et al. (2016).

The measurement requirements for the proposed estimation algorithm are summarized below.

- The speed of connected vehicles at any segment of the highway is measured and used for computing the average segment speed $v_i$, $i = 1, \ldots, N$, employed by the estimator.
- The flow of vehicles at the entry of the considered highway stretch, $q_0$, is available.
- The flow at the exit of the considered highway stretch, $q_N$, is available.

### 2.2.2 Kalman filter

A Kalman filter is utilized in order to estimate the traffic state of the network. Defining

$$\hat{x} = \left(\hat{\rho}_1, \ldots, \hat{\rho}_N\right)^T, \tag{2.12}$$

as the system state estimate, the filter equations are

$$\hat{x}(k+1) = A(k)\hat{x}(k) + Bu(k) + A(k)K(k)\left(z(k) - C\hat{x}(k)\right) \tag{2.13}$$

$$K(k) = P(k)C^T\left(CP(k)C^T + R\right)^{-1} \tag{2.14}$$

$$P(k+1) = A(k)\left(I - K(k)C\right)P(k)A(k)^T + Q, \tag{2.15}$$

where measurement $z$ is a noisy version of $y$ and $Q = Q^T > 0$ and $R = R^T > 0$ are tuning parameters which, in the ideal case in which there is additive, zero-mean Gaussian white noise in the state and output equations, represent the covariance matrices of the process and measurement noise, respectively. The initial conditions of the filter described by (2.13)–(2.15) are

$$\hat{x}(k_0) = \mu \tag{2.16}$$

$$P(k_0) = H, \tag{2.17}$$

where $\mu$ and $H = H^T > 0$, in the ideal case when $x(k_0)$ is a Gaussian random variable, represent the mean and auto covariance matrix of $x(k_0)$, respectively.

### 2.2.3 Case of unmeasured flow at on-ramps and off-ramps

In case the flows at some on-ramps or off-ramps of the highway stretch are not directly measured, these flows are considered as additional unmeasured states to be estimated by the Kalman filter. This way, the state (2.5) is alterated to

$$x = (\rho_1, \ldots, \rho_N, \theta_1, \ldots, \theta_{l_r+l_s})^T, \tag{2.18}$$

where $l_r$ and $l_s$ are the number of unmeasured flows at on-ramps and off-ramps, respectively, and

$$\theta_i = \begin{cases} \frac{T}{\Delta_i} r_{n_i}, & \text{if } n_i \in L_r \\ \frac{T}{\Delta_i} s_{n_i}, & \text{if } n_i \in L_s \end{cases}, \tag{2.19}$$

for all $i = 1, \ldots, l_r+l_s$, with $L_r = \{n_1, \ldots, n_{l_r}\}$ and $L_s = \{n_{l_r+1}, \ldots, n_{l_r+l_s}\}$ being the sets of segments, denoted by $n_i$, which have an on-ramp or an off-ramp, respectively, whose flows are not directly measured. Assuming that the unmeasured on-ramp and off-ramp flows are constant (or, effectively, slowly varying), the unmeasured ramp flow dynamics may be reflected by a random walk, i.e.,

$$\theta_i(k+1) = \theta_i(k) + \xi_i^\theta(k) \tag{2.20}$$

where $\xi_i^\theta$ is zero-mean white Gaussian noise. It is assumed that at a segment $i$ there can be either only one on-ramp or only one off-ramp, which is typically the case on a highway, and hence, $L_r \cap L_s = \emptyset$.

In this case, the deterministic part of the dynamics of the density given in (2.3) and of $\theta_i$ given in (2.20) can be written as

$$x(k+1) = A(k)x(k) + Bu(k), \tag{2.21}$$

where

$$A(k) = \begin{cases} a_{ij} = \frac{T}{\Delta_i} v_{i-1}(k), & \text{if } i-j=1 \text{ and } i \geq 2 \\ a_{ij} = 1 - \frac{T}{\Delta_i} v_i(k), & \text{if } i = j \\ a_{n_i j} = 1, & \text{if } n_i \in L_r \text{ and } j = N+i \\ a_{n_i j} = -1, & \text{if } n_i \in L_s \text{ and } j = N+i \\ a_{ij} = 1, & \text{if } N < i \leq N_1 \text{ and } j = i \\ a_{ij} = 0, & \text{otherwise} \end{cases} \tag{2.22}$$

$$B = \begin{cases} b_{ij} = \frac{T}{\Delta_i}, & \text{if } i = 1 \text{ and } j = 1 \\ b_{m_i j} = \frac{T}{\Delta_{m_i}}, & \text{if } m_i \notin \bar{L},\ 1 \leq m_i \leq N,\ 1 \leq i \leq N_2, \\ & \text{and } j = i+1 \\ b_{ij} = 0, & \text{otherwise} \end{cases} \tag{2.23}$$

$$u(k) = \begin{cases} u_i = q_0(k), & \text{if } i = 1 \\ u_{i+1} = r_{m_i} - s_{m_i}, & \text{if } m_i \notin \bar{L} \end{cases}, \tag{2.24}$$

with $\bar{L} = L_r \cup L_s$, $N_1 = N + l_r + l_s$, $N_2 = N - l_r - l_s$, $A \in \mathbb{R}^{N_1 \times N_1}$, $B \in \mathbb{R}^{N_1 \times (N_2+1)}$. The measured outputs associate with system (2.21)–(2.24) are the density (or equivalently, the flow) at the mainstream exit of the highway and at highway segments between any pair of unmeasured on-ramps and off-ramps, which can be obtained by fixed flow sensors via

$$\rho_j = \frac{q_j}{\upsilon_j}, \tag{2.25}$$

where $\upsilon_j$ is the speed of segment $j$ as reported by connected vehicles and $q_j$ is the corresponding flow of segment $j$, measured via a flow detector. Therefore,

$$y(k) = Cx(k), \tag{2.26}$$

where $C \in \mathbb{R}^{(l_r+l_s)\times(N+l_r+l_s)}$ is defined as

$$C = \begin{cases} c_{ij} = 1, & \text{for all } i = 1, \ldots, l_r + l_s - 1 \text{ and some } n_i^* \leq j \leq n_{i+1}^* - 1 \\ c_{ij} = 1, & \text{if } i = l_r + l_s \text{ and } j = N \\ c_{ij} = 0, & \text{otherwise} \end{cases} \tag{2,27}$$

where $\bar{L}^* = \left\{n_1^*, n_2^*, \ldots, n_{l_r+l_s}^*\right\}$ is the set $\bar{L}$ ordered by $<$. If there is exactly one unmeasured ramp within the considered highway stretch, then no additional measurements are necessary for flow observability. On the other hand, if there are more than one unmeasured ramps within the stretch, one mainstream measurement at any highway segment is needed, say $j$, between every two consecutive unmeasured ramps.

# Chapter 3

# Microscopic simulation setup for testing the proposed traffic estimation methodology

In order to thoroughly examine the effectiveness, sensitivity and further aspects of the scheme described in Section 2.2 in a microscopic environment, the microscopic traffic simulation software Aimsun by Transport Simulation Systems (Transport Simulation Systems, 2014) is employed. In particular, the features provided by Aimsun API and microSDK are exploited to extract data and results of the simulation or configure the simulation parameters and vehicle models. The default car-following model implemented by Aimsun is Gipps model (Gipps, 1981, 1986), which is used to model the dynamics of regular and connected vehicles without ACC capabilities. The setup of the microscopic simulation-based testing of the proposed estimation methodology is shown in Fig. 3.1. Upstream demand and on-ramp flow data are fed to the microscopic model along with certain parameters; based on which the model produces the traffic conditions of the employed scenarios. Specific traffic measurements are produced via realistically emulated detection procedures and are provided to the Kalman filter, whose parameters have been appropriately tuned; the Kalman filter then estimates the desired traffic quantity, namely $\rho_i$, which may be confronted to the "ground truth" of the simulator.

## 3.1 Traffic network configuration

For the evaluation of the estimation procedure, a highway stretch of 10 km is utilized, as shown in Fig. 3.2. The stretch has 3 lanes and is divided into 20 homogenous segments. Three on-ramps and three off-ramps are positioned at segments 8, 12, 16

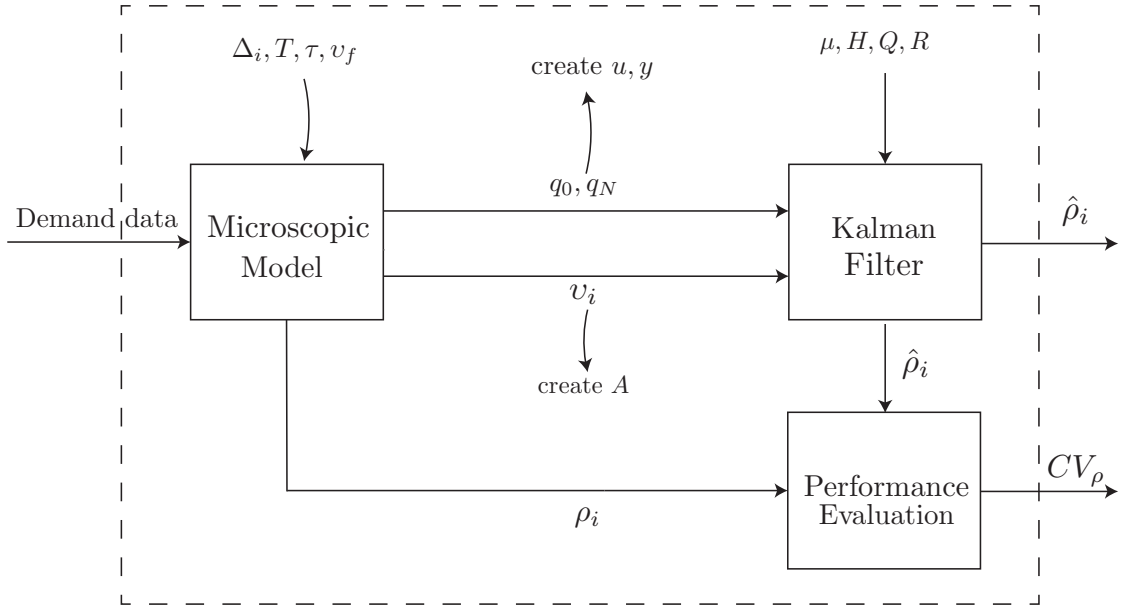


Fig. 3.1: Setup of the microscopic simulation-based testing environment for the proposed estimation methodology.

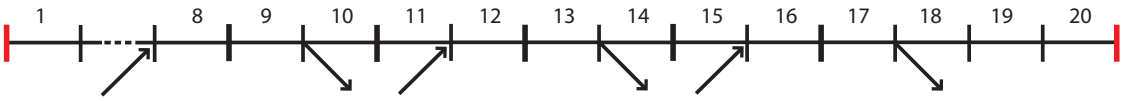


Fig. 3.2: The highway stretch used in the experiment. Red vertical lines indicate fixed flow sensors positioned at the network entry and exit.

and 10, 14, 18, respectively; acceleration lanes at on-ramp locations and deceleration lanes at off-ramp locations are 100 m in length. The utilized network parameters are summarized in Table 3.1.

## 3.2 Employed scenario

For the purpose of testing the estimation scheme in free-flow as well as congested traffic conditions, a 3-hour simulation horizon is employed, setting the simulation

| Network length (km) | Number of segments N | Number of lanes | Segment length $\Delta_i$ (km) | Free speed $v_f$ (km/h) |
|---|---|---|---|---|
| 10 | 20 | 3 | 0.5 | 120 |

Table 3.1: Network parameter values

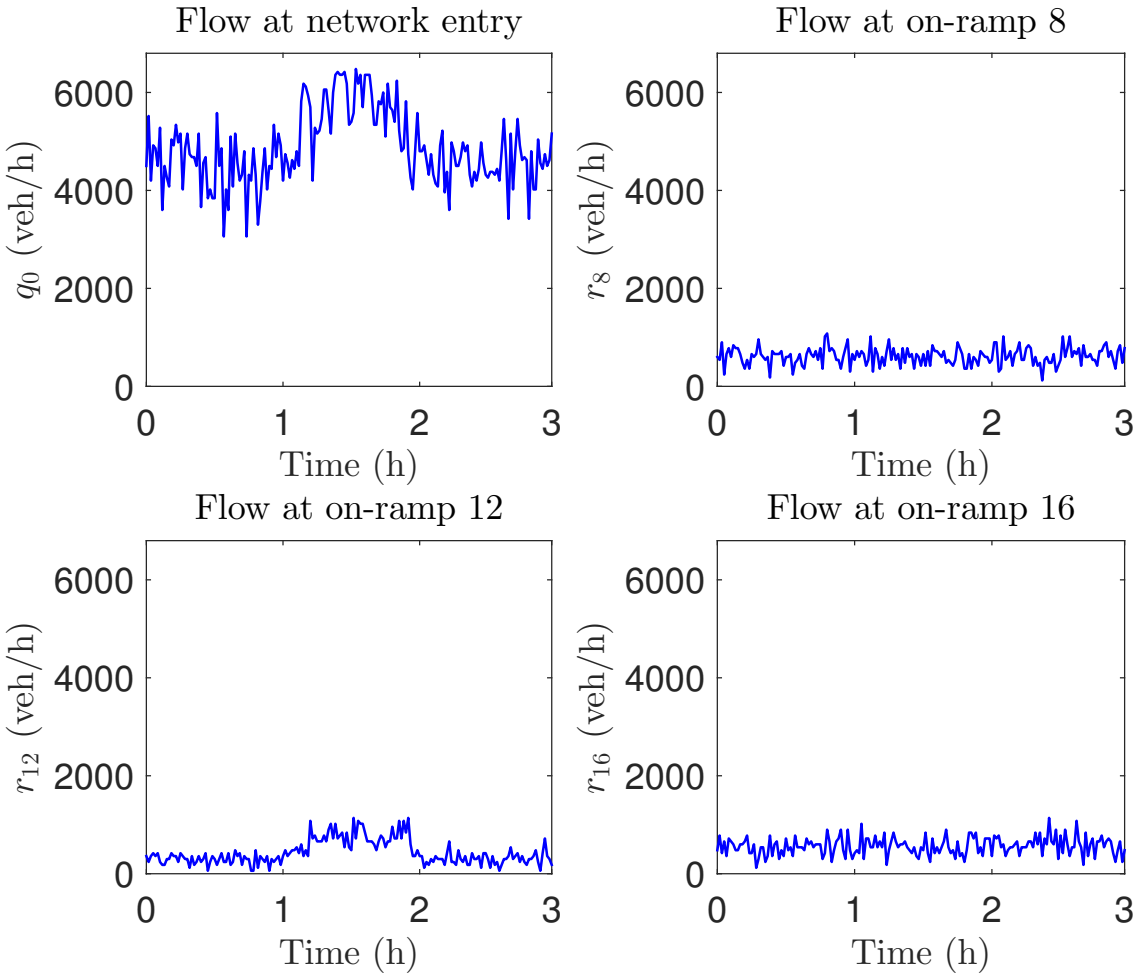


Fig. 3.3: The inflow at the entry of the highway stretch and the on-ramp flows at segments 8, 12, and 16.

step as well as the reaction time of all vehicles $\tau$ at 1 s. Inflows at the network entrance and at on-ramps are the product of an exponential distribution, with a specified mean value. The inflow at the network entrance $q_0$ is chosen, on average, as trapezoidal. The on-ramps at segments 8 and 16 feature, on average, a constant flow of 600 veh/h for the whole simulation time; whereas the on-ramp flow at segment 12 is also on average trapezoidal. The demand profiles are shown in Fig. 3.3. Turning rates at each off-ramp are constant at 10% of the mainstream flow of the corresponding segment.

## 3.3 Measurement and ground truth configuration

A measurement step $T = 10$ s is considered, which corresponds to the detection interval of flow sensors, as well as the interval for calculating average segment speeds.

A conventional spot sensor is placed at the entrance of the network, providing measurements of inflow $q_0$, whereas an additional spot sensor is placed at the exit of the network, providing measurements of the outflow $q_{20}$. All flows are computed by counting the number of vehicles that cross the corresponding detector within the time interval $(kT, (k+1)T]$. Segment speed is computed by averaging arithmetically the instant speed of all vehicles in a segment at time step $kT$. The ground truth in our experiments, considered for evaluating the performance of the proposed estimation scheme, is represented by the total density of each segment, calculated by dividing the number of vehicles in a segment at time $kT$ with the segment length (0.5 km).

# Chapter 4

# Estimation results in the case of all ramps being measured

## 4.1 Experimental configuration

The traffic network and employed scenario described in Section 3 are considered to simulate a case featuring traffic conditions where all vehicles are connected, in order to test the performance of the estimation scheme. Given that the microscopic model parameters are stochastic (such as demand, destination, and vehicle attributes), 10 simulation replications are considered. Fig. 4.1 shows the traffic conditions for the scenario described . For the first hour, the inflows at the entry of the network and at all on-ramps are low, as presented in Fig. 3.3, and thus, free-flow conditions are present in the whole network. During the second hour, the flows at the network entrance and at on-ramp 12 start increasing. As a result, congestion is created at segment 12 and segment 8, which propagates upstream reaching segment 4. Mild congestion is also created in segment 16, where the third on-ramp is present. At the beginning of the third hour of the simulation, since the inflows at the network entry and at on-ramp 12 are decreased, congestion gradually dissolves, and free-flow conditions are restored until the end of the simulation time, as shown in Fig. 4.1.

In order to evaluate the estimation results, the following performance index, known as Coefficient of Variation (CV) of the estimated density $\hat{\rho}_i$ with respect to the ground truth density $\rho_i$, is used

$$CV_\rho = \frac{\sqrt{\frac{1}{KN}\sum_{k=1}^{K}\sum_{i=1}^{N}[\hat{\rho}_i(k) - \rho_i(k)]^2}}{\frac{1}{KN}\sum_{k=1}^{K}\sum_{i=1}^{N}\rho_i(k)}. \tag{4.1}$$

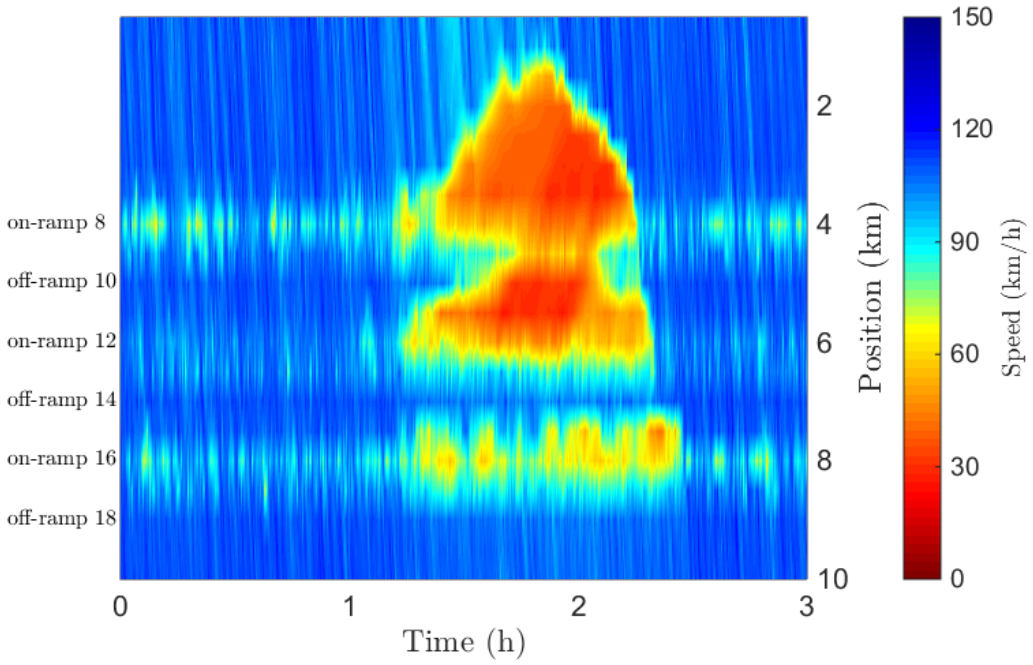


Fig. 4.1: Average speed of all vehicles in the employed simulation scenario.

## 4.2 Performance evaluation in the case of all vehicles being connected

In order to select the values of the filter parameters $Q$ and $R$ used in our experiments, a manual tuning is performed, and the results are shown in Table 4.1. Matrix $Q$ is chosen be equal to $I_N$, where $I_N$ denotes the identity matrix of dimension $N$, while $R$ is chosen equal to 100; initial values $\mu$ are chosen equal to 15, whereas $H$ is equal to $I_N$. The parameters $\mu$ and $H$ are given by (2.16), (2.17), respectively. The results of the estimation of segment densities when all vehicles are connected are shown in Fig. 4.2. It is evident from the plots that the proposed scheme successfully estimates and dynamically tracks segment densities under various traffic conditions, that is, under both congested and free-flow conditions. Note also the fast convergence of the estimates towards the real values, starting from remote initial values, which were deliberately chosen far from the real values in order to test the filter's convergence properties. The segment density estimation is characterized by a performance index $CV_\rho = 9.2\%$. Note that (4.1) is employed after the initial transient period of 20 minutes (due to the initial estimation error) to ensure that this period is excluded from the computation of the performance indexs.

| $Q$ | $R$ | $\mu$ | $H$ |
|---|---|---|---|
| $I_N$ | 100 | $(15, \ldots, 15)^T$ | $I_N$ |

Table 4.1: Filter parameters used in the simulation in the case that all ramps are measured.

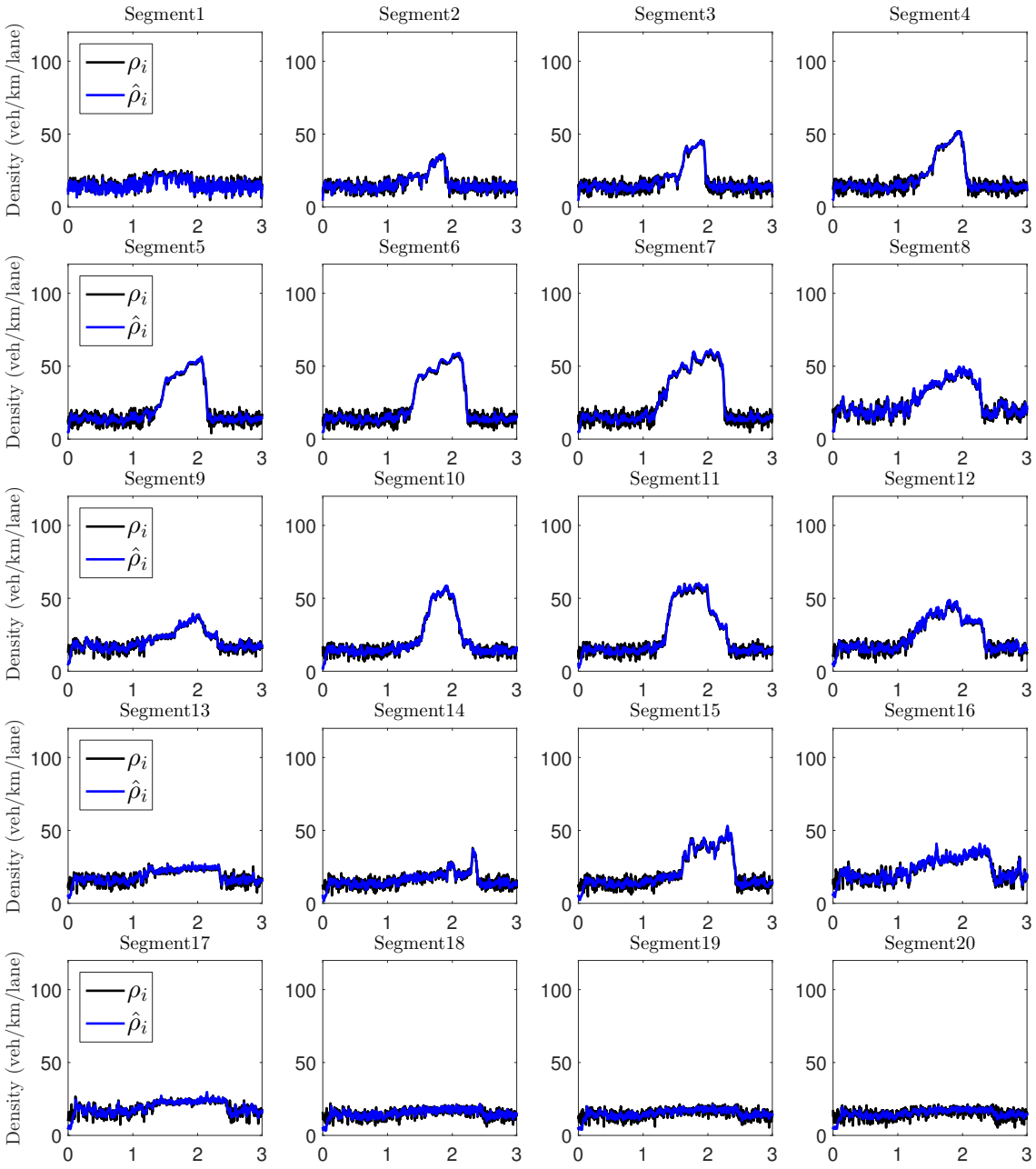


Fig. 4.2: Comparison between real (black line) and estimated (blue line) density per lane in veh/km for all network segments in the case that all vehicles are connected.

## 4.3 Performance evaluation in the case of all vehicles being connected featuring delayed speed reports

In this section, the performance of the estimation scheme is tested when the speed fed to the filter is delayed by some time steps. The values of the filter parameters are the same as in Section 4.2 and are shown in Table 4.1. The estimation performance is tested when the speed that is used by the filter is delayed by 3 time steps, i.e., $v_i(k) = \nu_i(k-3)$, where $v_i(k)$ is the speed that is utilized by the filter at time step $kT$ and $\nu_i(k)$ is the speed calculated from connected vehicle reports at time step $kT$. The results are shown in Fig. 4.3 and density estimation is characterized by a $CV_\rho = 14.9$. The plots show very little deterioration of the density estimation, however the deterioration caused by the delay in the speed measurements is more reflected in the value of the performance index $CV_\rho$.

## 4.4 Performance evaluation when connected vehicles feature asynchronous speed reports

In this section, an alternative speed reporting scheme for the speed stemming from connected vehicles is considered, in order to simulate a more realistic scenario. Segment speeds are derived from reports of a sub-population of the vehicles that are connected and hence, have the ability to report their position and instant speed to the central authority at a specific frequency. In order for the reporting scheme to be more realistic, "asynchronous" reports are considered, that is, vehicles report their speeds at different frequencies. This is implemented as follows. Upon entering the network, connected vehicles are assigned randomly a reporting frequency $f$, taken from a uniform distribution over the interval $[0.1, 1]$ Hz. This way, at every simulation step (1 s), only a portion of connected vehicles report their instant speed, depending on their reporting frequency. Eventually, all individual instant speed reports of connected vehicles from each segment within time interval $((k-1)T, kT]$ are averaged arithmetically and provide the average segment speed at time $kT$, namely, $v_i(k)$. Note that individual reports are considered as distinct measurements regardless of the vehicle that is reporting. This way, within an interval of $T = 10$ s, a vehicle that reports every 1 s, supplies the central authority with more measurements than a vehicle that reports every 9 s, thus contributing more in the calculation of the corresponding average segment speed. In order to assess the accuracy of speed

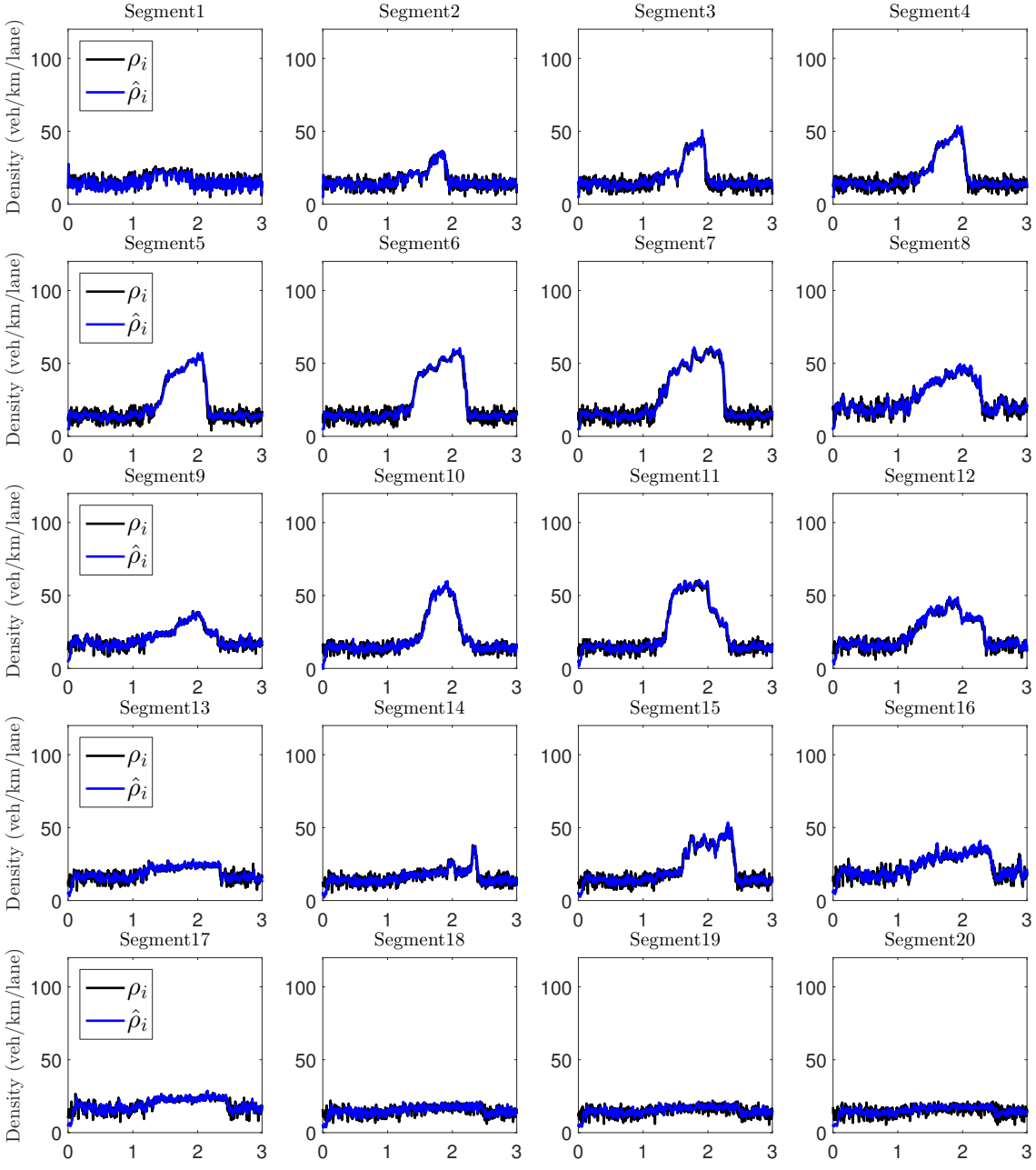


Fig. 4.3: Comparison between real (black line) and estimated (blue line) density per lane in veh/km for all network segments in the case that all vehicles are connected and the speed fed to the filter is delayed by 3 time steps.

measurements from connected vehicles, the result of averaging instant speeds of all segment vehicles every 1 s and then obtaining the average for $T = 10$ s is considered as ground truth.

Results of density estimation when using asynchronous speed reports are shown in Fig. 4.4. One can observe in the plots that implementing a more realistic reporting scheme with asynchronous reports from connected vehicles does not deteriorate the estimation performance significantly. The performance index of density estimation with the alternative reporting scheme is equal to 10.7%, indicating that the deterioration in the estimation performance is substantially small. For the rest of the text connected vehicles are considered to report according to the asynchronous reporting scheme described in this section.

## 4.5 Performance evaluation when speed reports from connected vehicles are subject to measurement noise

In order to simulate a more realistic approach, since all measurements produced by the simulation are error-free, a zero-mean Gaussian white measurement noise is added to all measurements. Thus, mainstream flow measurements as well as individual vehicle speed measurements obtained from connected vehicles are affected by additive noise with a Standard Deviation (SD) shown in Table 4.2. Considering the speed measurement accuracy of GPS mentioned in Section 2.1, adding noise with an SD of 5 km/h is a realistic choice, which in fact covers the worst-case scenario. Moreover, the GPS positional error, which could potentially result in a decreased speed measurements accuracy due to an erroneous determination of the segment that a vehicle is on, is, as mentioned in Section 2.1, extremely small compared to the length of a segment, and thus, its effect on the estimation performance is deemed negligible. Note that in case the transmitting device is also connected with the vehicle's electronic system, the speed measurements can be retrieved from the tachometer, whose measurements are substantially more accurate (Zito et al., 1995) (resulting in a smaller SD of the speed measurement error). However, an error that is representative of GPS devices is chosen, since devices equipped with GPS (e.g., smartphones, navigation systems) are perhaps the most widespread devices that enable the acquisition of speed information by the central authority (Bishop, 2005). Thus, since GPS feature larger measurement error than tachometers, the performance of the estimation in worst-case-error scenarios is actually tested. As for

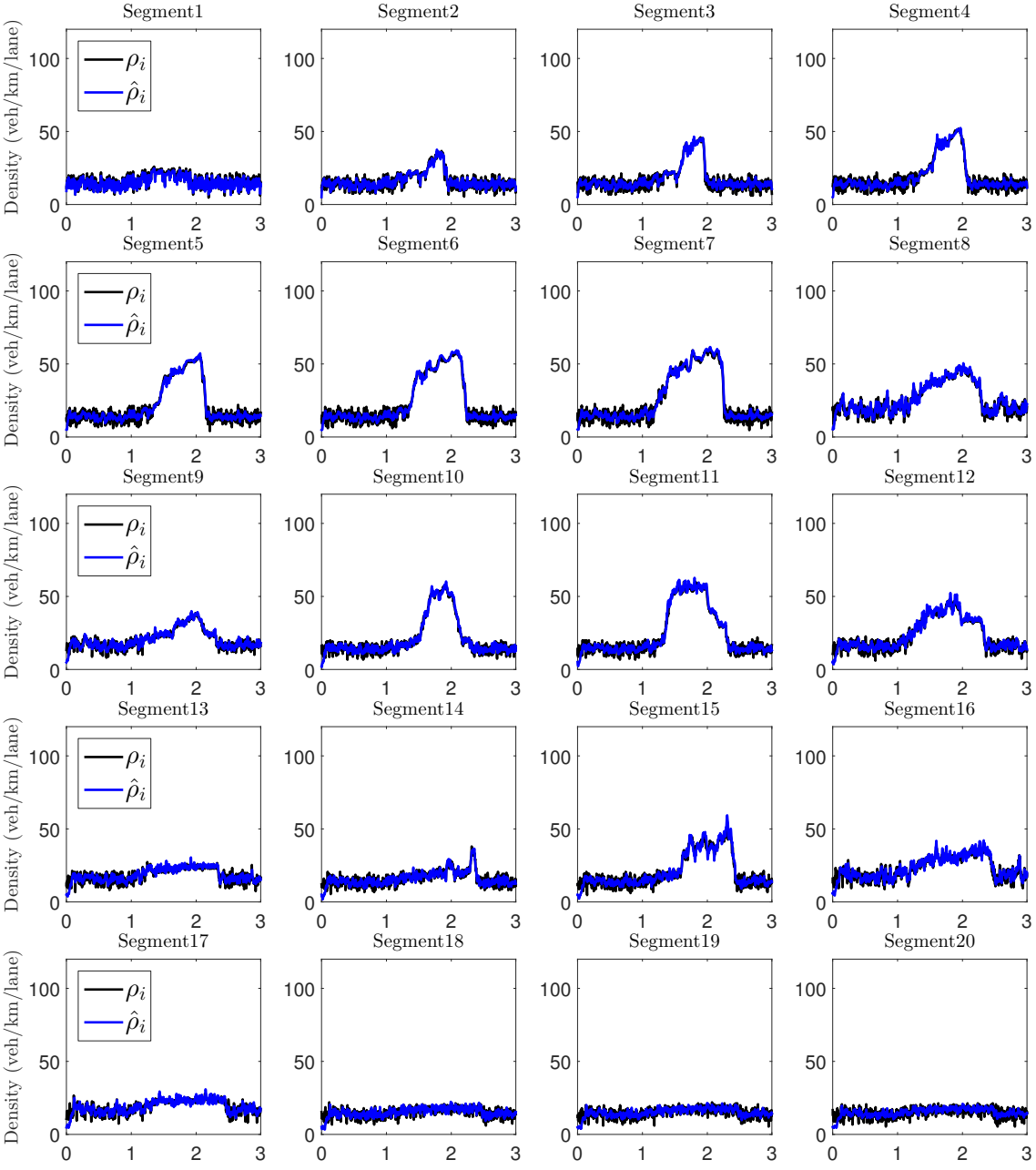


Fig. 4.4: Comparison between real (black line) and estimated (blue line) density per lane in veh/km for all network segments in the case that all vehicles are connected and their speeds are reported asynchronously.

| Noise | $\gamma_i^q$ | $\gamma_i^r$ | $\gamma_i^s$ | $\gamma_i^v$ |
|---|---|---|---|---|
| SD | 500 veh/h | 60 veh/h | 60 veh/h | 5 km/h |

Table 4.2: Measurement noise (SD) of individual vehicles speed reported by connected vehicles and of mainstream and ramp flow gathered by spot sensors.

the infrastructure-based mainstream flow sensors, an error of about 10% is reported to be realistic, see, e.g., Yue (2009). Since the average inflow is around 5000 veh/h and the average ramp flow is around 600 veh/h an error with an SD of 500 veh/h for mainstream flows and 60 veh/h for ramp flows is considered.

Results of density estimation when zero-mean Gaussian white measurement noise is added to flow and speed measurements are shown in Fig. 4.5. The results do not show any significant difference with the case that all measurements are noise-free, allowing us to consider a more realistic scenario without having a considerably negative result in the performance of the estimation scheme. The performance of the estimation when noise is added to the speed and flow measurements is characterized by a performance index $CV_\rho = 11.1\%$, while the performance index of the estimation with noise-free measurements was characterized by a performance index $CV_\rho = 10.7$. All simulations for the rest of the text will be considered to include measurement noise.

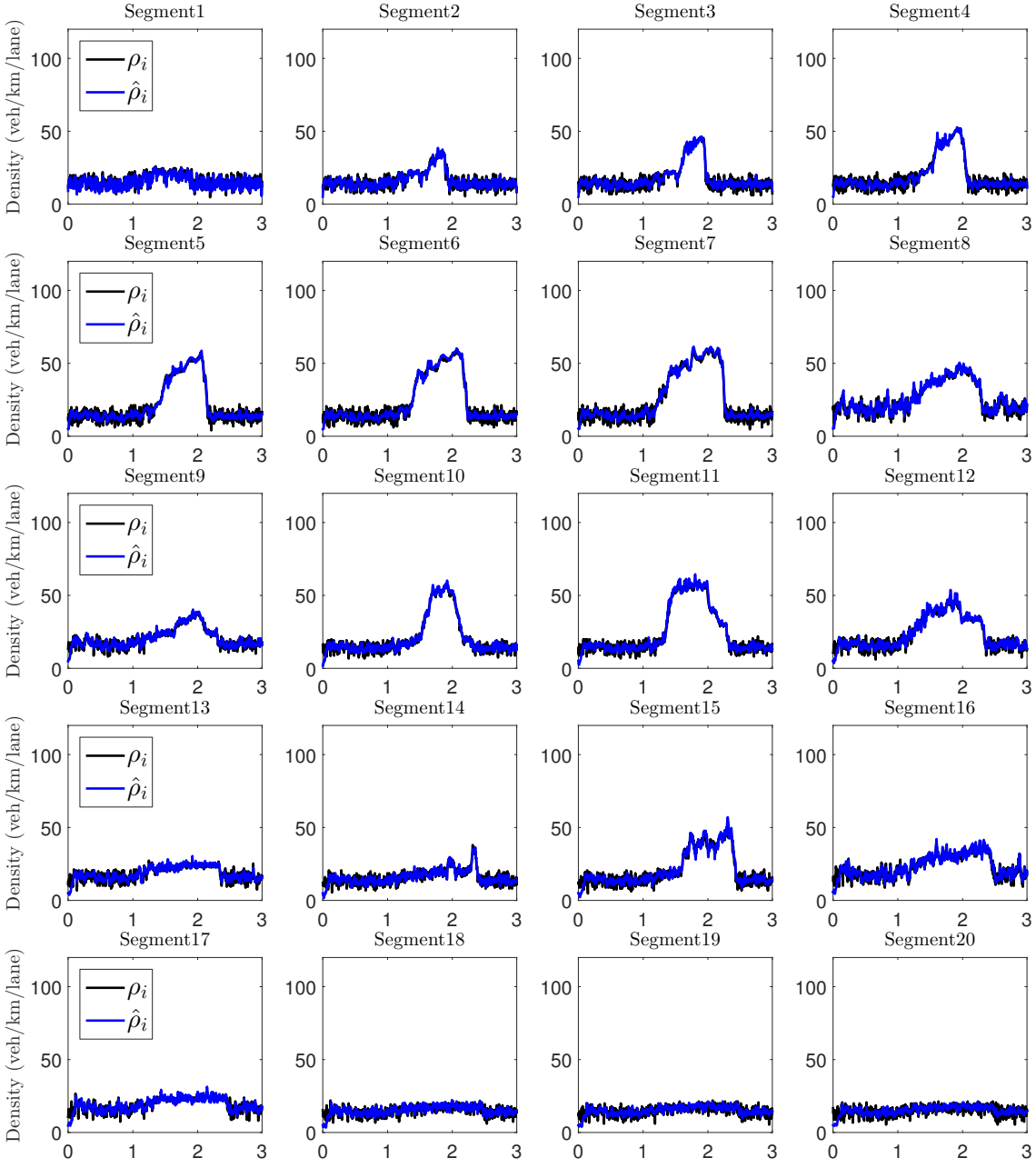


Fig. 4.5: Comparison between real (black line) and estimated (blue line) density per lane in veh/km for all network segments in the case that all vehicles are connected and there is noise in flow and speed measurements.

# Chapter 5

# Estimation results in the case of unmeasured ramps

## 5.1 Experimental configuration

In this section the case of specific ramps in the network being unmeasured is tested, utilizing the scheme described in Section 2.2.3. The estimation methodology is described in Fig. 5.1 and the network configuration is shown in Fig. 5.2. Depending of the number of unmeasured ramps, additional spot sensors may need to be placed between subsequent unmeasured ramps in order to guarantee the observability of the system (see Bekiaris-Liberis et al. (2016)), as described in Section 2.2. Regarding the ground truth for the estimated ramp flows, since flows calculated in time intervals as small as 10 s are very oscillatory, a moving average of the last 6 flow measurements is considered as ground truth.

In order to evaluate the estimation results for unmeasured ramp flows, the CV of the estimated on-ramp flow $\hat{r}_i$ and off-ramp flow $\hat{s}_i$, with respect to the ground truth on-ramp flow $r_i$ and off-ramp flow $s_i$, respectively, are given by the following equations

$$CV_r = \frac{\sqrt{\frac{1}{Kl_r}\sum_{k=1}^{K}\sum_{i=1}^{l_r}[\hat{r}_i(k) - r_i(k)]^2}}{\frac{1}{Kl_r}\sum_{k=1}^{K}\sum_{i=1}^{l_r} r_i(k)}, \tag{5.1}$$

$$CV_s = \frac{\sqrt{\frac{1}{Kl_s}\sum_{k=1}^{K}\sum_{i=1}^{l_s}[\hat{s}_i(k) - s_i(k)]^2}}{\frac{1}{Kl_s}\sum_{k=1}^{K}\sum_{i=1}^{l_s} s_i(k)}. \tag{5.2}$$

Additionally, for evaluating the total unmeasured ramp flows estimation performance, total CV of the estimated ramp flow $\frac{\Delta_i}{T}\hat{\theta}_i$ (see (2.19)) with respect to the

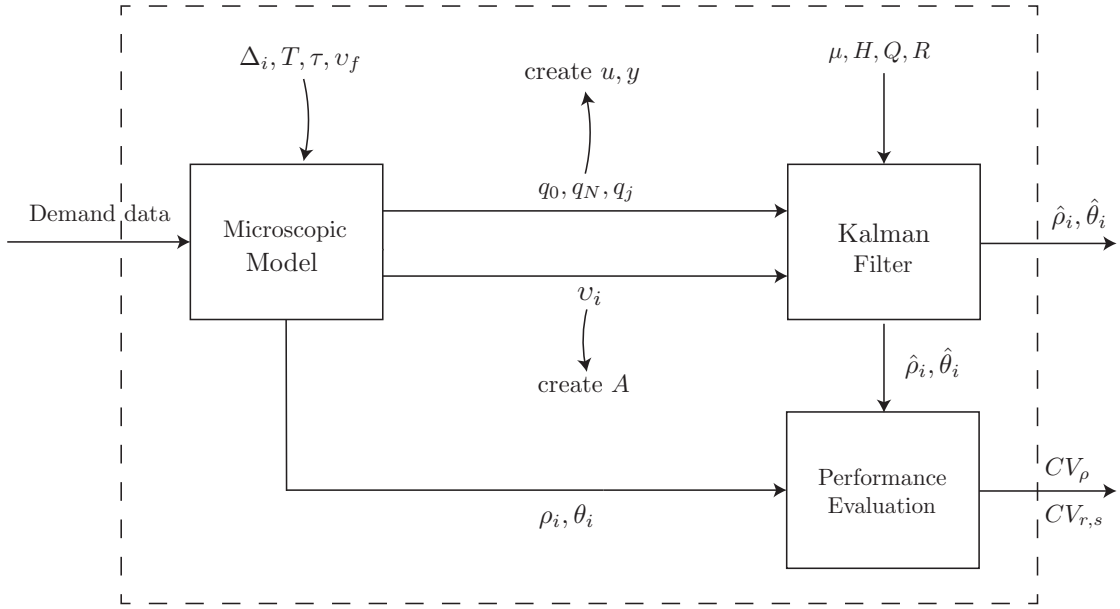


Fig. 5.1: Setup of the microscopic simulation-based testing of the proposed estimation methodology in the case that there are unmeasured ramps.

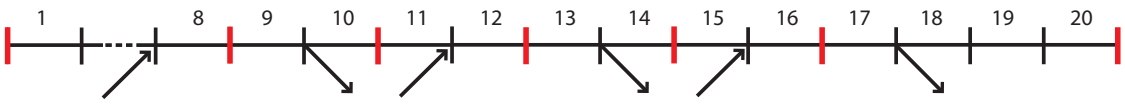


Fig. 5.2: The setup of the highway stretch in the case that there are unmeasured ramps. Red vertical lines indicate fixed flow sensors positioned at the network entry and exit as well as at the end of segments between subsequent ramps.

| $Q$ | $\sigma_\rho$ | $\sigma_{r,s}$ | $H$ |
|---|---|---|---|
| $\text{diag}(\sigma_\rho \times I_N, \sigma_{r,s} \times I_{(l_r+l_s)})$ | 1 | 0.1 | $I_{(N+l_r+l_s)}$ |
| $R$ | $\sigma_R$ | $\mu$ | |
| $\text{diag}(\sigma_R \times I_{(l_r+l_s)})$ | 100 | $(15, \ldots, 15, 5, \ldots, 5)^T$ | |

Table 5.1: Filter parameters used in the simulation in the case of unmeasured ramps.

ground truth ramp flow $\frac{\Delta_i}{T}\theta_i$, is used, given by the following equation

$$CV_{r,s} = \frac{\sqrt{\frac{1}{K(l_r+l_s)} \sum_{k=1}^{K} \sum_{i=1}^{l_r+l_s} {\Delta_i}^2 [\hat{\theta}_i(k) - \theta_i(k)]^2}}{\frac{1}{K(l_r+l_s)} \sum_{k=1}^{K} \sum_{i=1}^{l_r+l_s} \Delta_i \theta_i(k)}. \tag{5.3}$$

The entry of matrix $Q$ that corresponds to density is chosen to be $\sigma_\rho \times I_N$, where $I_N$ denotes the identity matrix of dimension $N$ and $\sigma_\rho$ is equal to 1, while the entry that corresponds to unmeasured ramps is chosen as $\sigma_{r,s} \times I_{(l_r+l_s)}$, where $\sigma_{r,s}$ is equal to 0.1. Similarly, matrix $R$ is chosen to be $\sigma_R \times I_{(l_r+l_s)}$, where $\sigma_R$ is equal to 100, as shown in Table 5.1. Additionally, the initial values $\mu$ that correspond to density are set equal to 15, while entries that correspond to unmeasured ramps are equal to 5; and $H = I_{(N+l_r+l_s)}$ (see (2.16), (2.17)); note that these initial values have some impact on the estimation results only at a short warm-up phase (when the filter is switched on), hence they are of minor significance.

## 5.2 Case of one unmeasured ramp

The performance of the estimation scheme is evaluated when the first on-ramp located at segment 8 is unmeasured . As described in Section 2.2, when there is only one unmeasured ramp there is no need for an additional detector since the system is still observable. The estimation results for densities and for the on-ramp flow are shown in Fig. 5.3 and Fig. 5.4, respectively. The performance index of density estimation is $CV_\rho = 11.2\%$ whereas for the estimation of on-ramp 8 the resulting performance index is $CV_{r,s} = 35.4\%$. It is evident from the plots as well as from the resulting performance indices that the density estimation is very satisfactory, almost identical with the case that all ramps are measured, whereas ramp flow estimation is also shown to be very satisfactory.

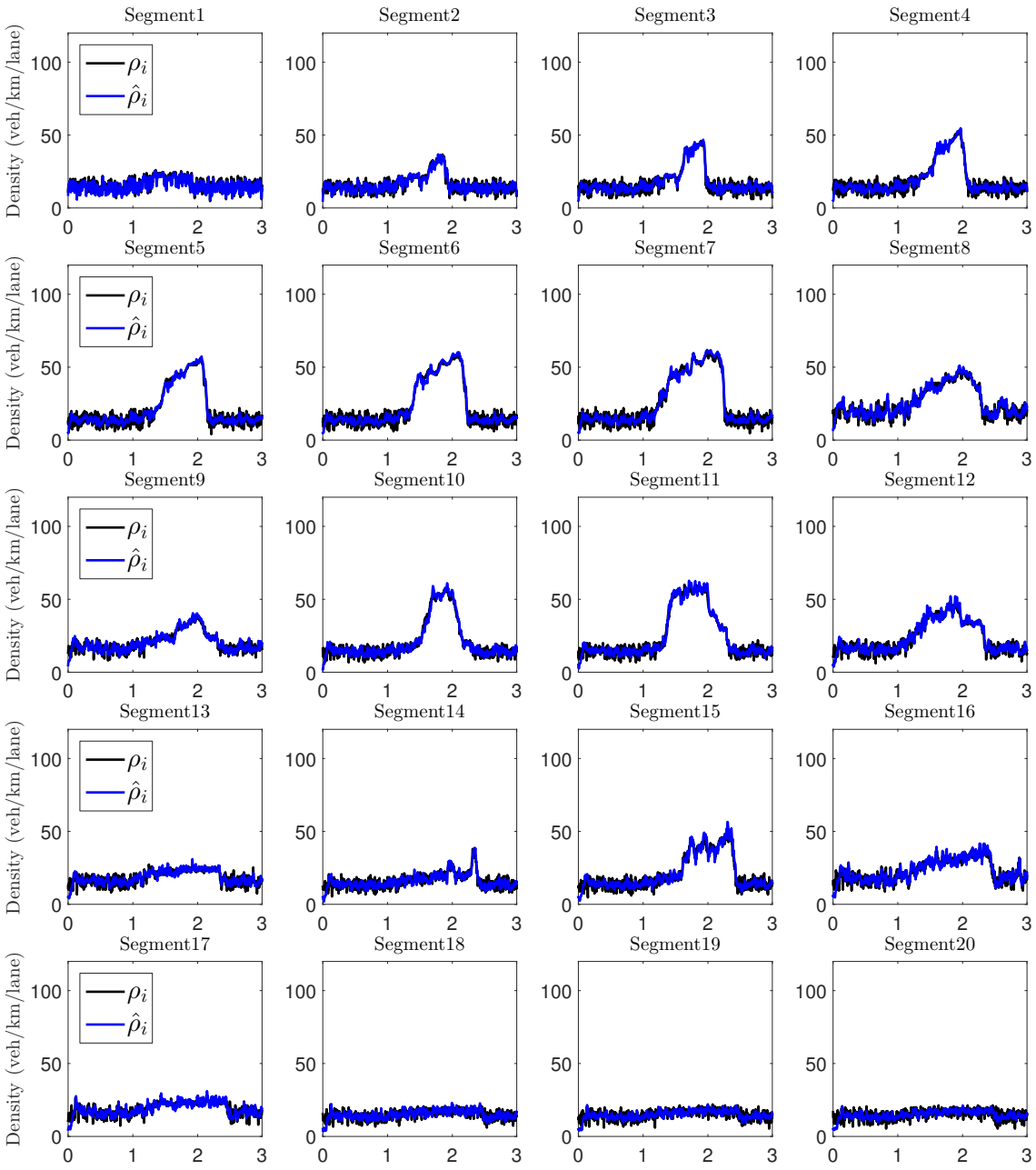


Fig. 5.3: Comparison between real (black line) and estimated (blue line) density per lane in veh/km for all network segments in the case that on-ramp 8 is unmeasured.

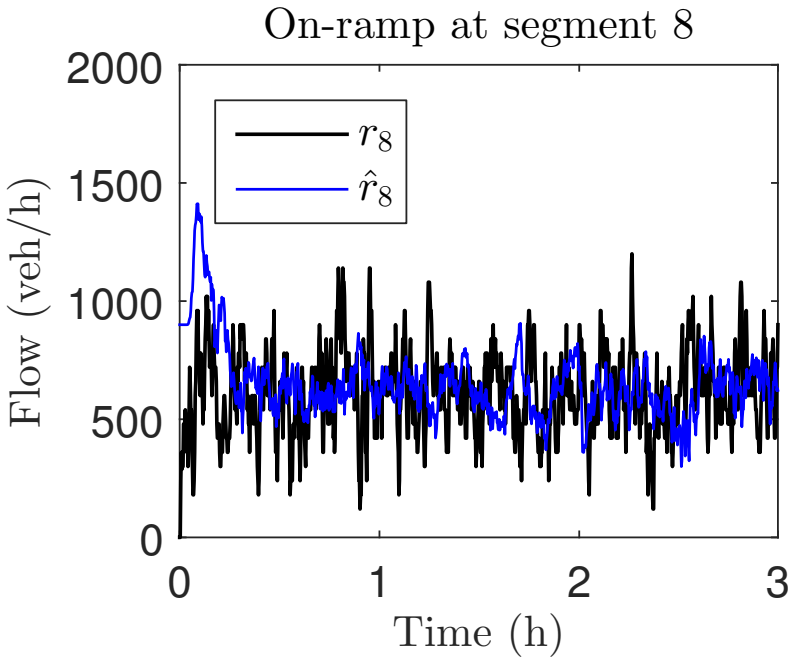


Fig. 5.4: Comparison between real (black line) and estimated (blue line) ramp flow in veh/h in the case that on-ramp 8 is unmeasured.

## 5.3 Case of two unmeasured ramps

In this section, the performance of the estimation scheme is evaluated for the case there are two unmeasured ramps. Consequently, the on-ramp at the location of segment 12 as well as the off-ramp at the location of segment 18 are considered unmeasured, whereas an additional flow sensor is placed at the location of segment 13, in order to guarantee the observability of the system, as described in Section 2.2. The resulting estimated densities and ramp flows are shown in Fig. 5.5 and Fig. 5.6, respectively. The performance index of density estimation is calculated equal to $CV_\rho = 10.9\%$, which is similar with the case of all ramps being measured as well as with the case that the on-ramp at the location of segment 8 is unmeasured. The total performance index for ramp flow estimation is calculated equal to $CV_{r,s} = 36.4\%$, whereas the performance index of the estimation of on-ramp 12 is $CV_r = 37.2\%$ and of off-ramp 18 is $CV_s = 35.6\%$, indicating that the estimation performance is similar for both ramps.

## 5.4 Case of all ramps being unmeasured

In this section, the estimation scheme is tested for the case that all ramps in the network, i.e., on-ramps at the locations of segments 8, 12, and 16 as well as off-

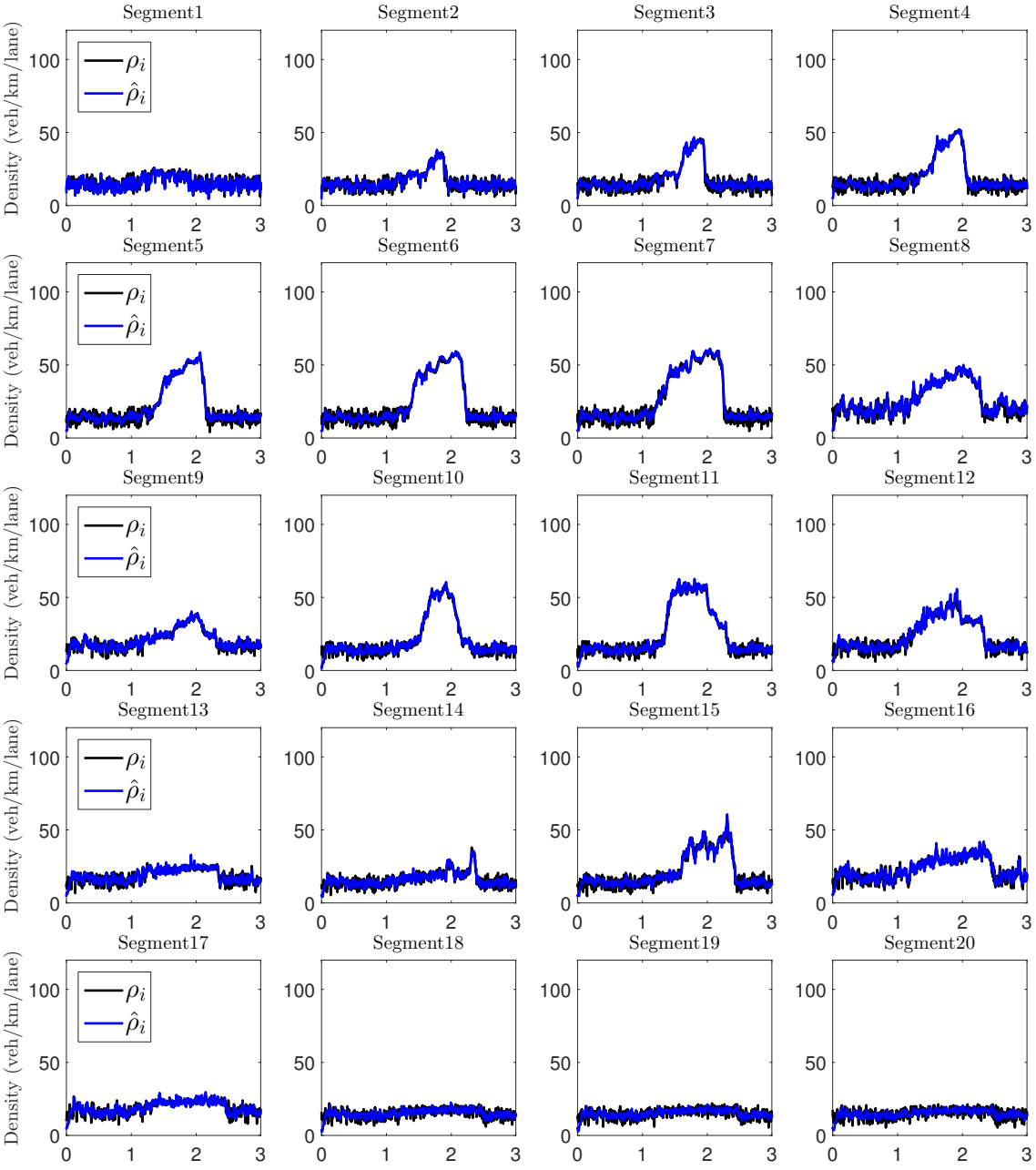


Fig. 5.5: Comparison between real (black line) and estimated (blue line) density per lane in veh/km for all network segments when on-ramp 12 and off-ramp 18 are unmeasured.

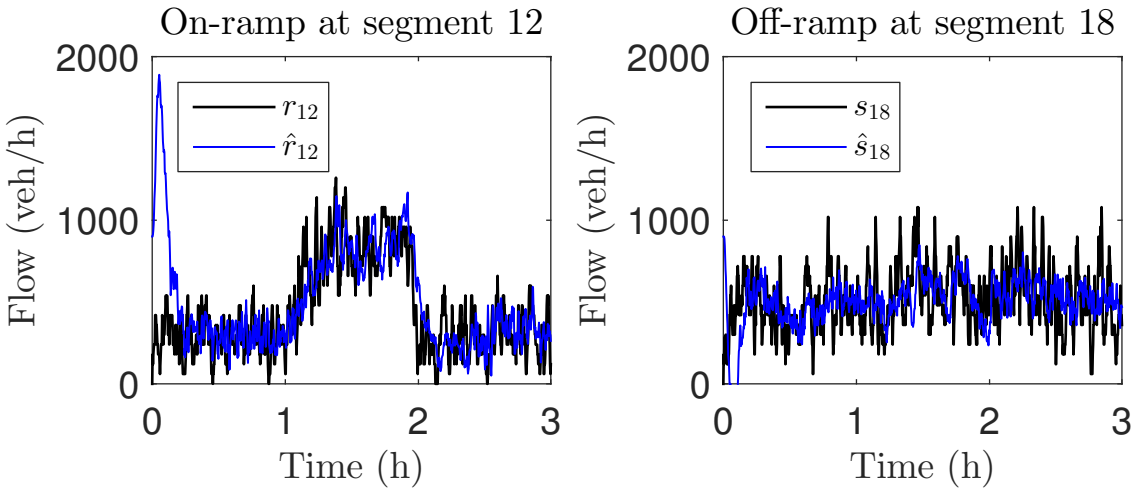


Fig. 5.6: Comparison between real (black line) and estimated (blue line) ramp flows in veh/h when on-ramp 12 and off-ramp 18 are unmeasured.

ramps at the locations of segments 10, 14, and 18 are considered unmeasured. In order for the system to be observable, 5 additional detectors need to be placed between every pair of subsequent unmeasured ramps, to provide measurements of the corresponding segment flow. Consequently, flow detectors are placed at the location of segments 8, 10, 12, 14, and 16 providing measurements of the flows $q_8$, $q_{10}$, $q_{12}$, $q_{14}$, and $q_{16}$, respectively. The results of density and ramp flow estimation are presented in Fig. 5.7 and Fig. 5.8, respectively, where it is evident that both density and ramp flow estimations are very satisfactory even when all ramps are considered unmeasured. Density estimation is characterized by a performance index $CV_\rho = 11.4\%$, whereas the estimation of all ramp flows is characterized by a performance index $CV_{r,s} = 38.3\%$. In particular, on-ramp 8 is characterized by a flow estimation performance index 36.2%, off-ramp 10 by 42.2%, on-ramp 12 by 41.9%, off-ramp 14 by 36.8%, on-ramp 16 by 34.6% and off-ramp 18 by 38.9%. In total, on-ramp flow estimation is characterized by a performance index $CV_r = 37.6\%$, whereas off-ramp flow estimation is characterized by a performance index $CV_s = 39.3\%$.

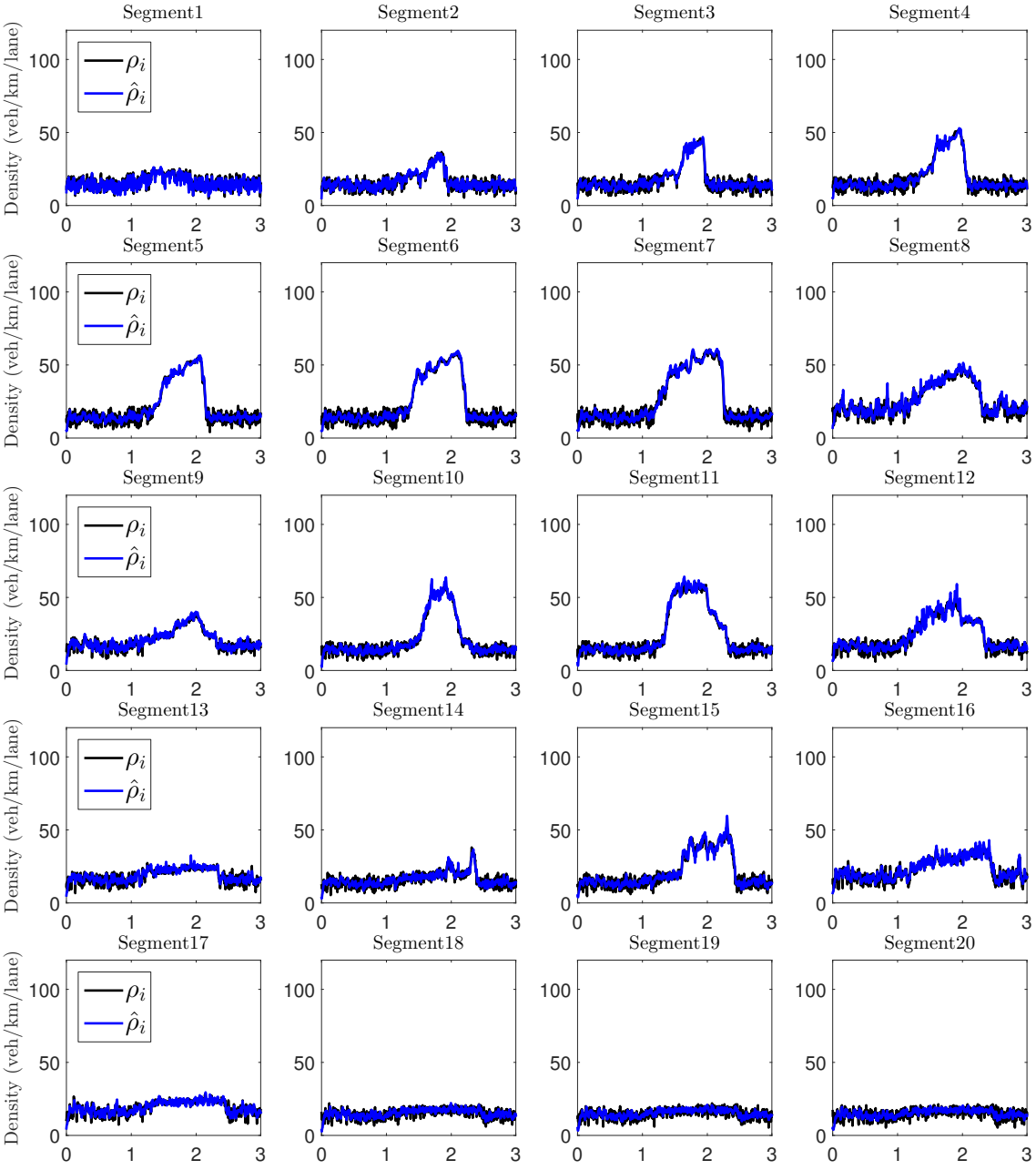


Fig. 5.7: Comparison between real (black line) and estimated (blue line) density per lane in veh/km for all network segments when all on-ramps and off-ramps in the network are unmeasured.

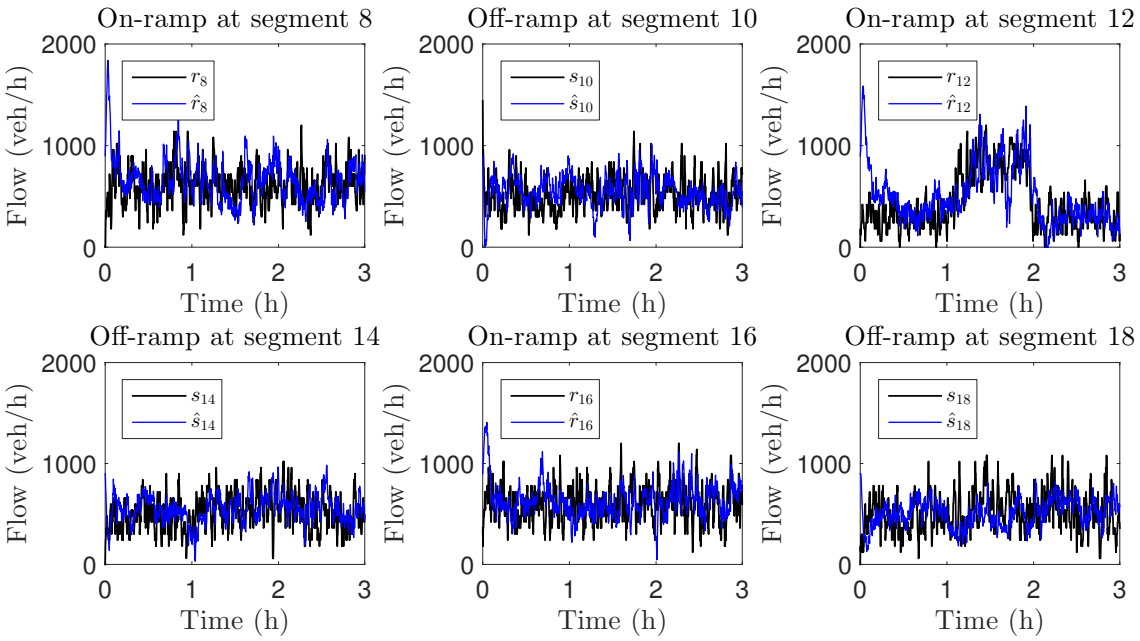


Fig. 5.8: Comparison between real (black line) and estimated (blue line) ramp flows in veh/h when all on-ramps and off-ramps in the network are unmeasured.

# Chapter 6

# Mixed traffic estimation results in the presence of regular and connected vehicles

## 6.1 Experimental configuration

In this chapter, the traffic network and scenario described in Section 5 is considered to simulate a case where all ramps are unmeasured considering mixed traffic conditions, i.e., traffic comprising conventional and connected vehicles. Within this chapter, the attributes of both types of vehicles, such as desired speed, maximum acceleration and deceleration etc., are given by a distribution with the same mean and SD, and as a result, their overall behaviour is identical. The performance of the estimation scheme is evaluated next for a variety of penetration rates of connected vehicles. Currently, the penetration rate of connected vehicles is quite low, however it is expected to increase substantially in the future (Diakaki et al., 2015). To account for a variety of possible current and future traffic scenarios, the performance of the estimation scheme is evaluated for a wide range of penetration rates of connected vehicles, more specifically, 2%, 5%, 10%, 20%, and 50%. Given that the microscopic model parameters are stochastic (such as demand, destination, and vehicle attributes),10 simulation replications are considered for each penetration rate.

## 6.2 Computation of the measurements utilized by the estimator

As mentioned in Section 2.2, the estimation scheme is developed based on the assumption that the average of connected vehicles speed roughly equals the average of conventional vehicles speed. Since the driving statistics for all vehicles (connected or not) are the same, this assumption implies that the average speed of a small sample (depending on the penetration rate) of (connected) vehicles is representative for the average speed of the whole vehicle population in a segment. The accuracy of this assumption depends on the variance of individual vehicle speeds, e.g. in dependence of the average speed, see e.g., Garber and Gadirau (1989). In this section, this issue is investigated within our simulation setup in order to gain some insights on the accuracy level of the assumption above.

When calculating the average segment speed from reports by connected vehicles, two are the main problems that may degrade the estimation performance:

- For low penetration rates, when only few vehicles are present in a segment, the individual speed reports may be non-representative of the overall segment speed, due to, for example, an accidental vehicle breaking or stopping at the time of the report; or because all reports happen to originate from vehicles driving in a slow or in a fast lane, which would be lower or higher, respectively, compared to the average speed of vehicles in all lanes.

- In some cases, a low penetration rate may result in no connected vehicle being present in a segment during a time interval of $T = 10$ s. Fig. 6.1 shows the percentage of time intervals of $T = 10$ s that feature no connected vehicle report, averaged over all segments and replications. It is evident from Fig. 6.1 that for penetration rates of 10% or lower a substantial percentage of time intervals are bare of reports from connected vehicles. In fact, this percentage reaches 50% for a penetration rate of 2%. In such cases, since there is no information available about the current segment speed, a possible option is to employ measurements reported for the same segment during previous time intervals.

In order to obtain information about the actual difference between the ground truth average segment speeds and the average speeds computed by connected vehicles reports, Fig. 6.2 shows the error between the ground truth speed and the speed of connected vehicles for a 20% penetration rate. It is evident that the difference in speed in terms of SD is lower in high (i.e., when free-flow conditions prevail) and low

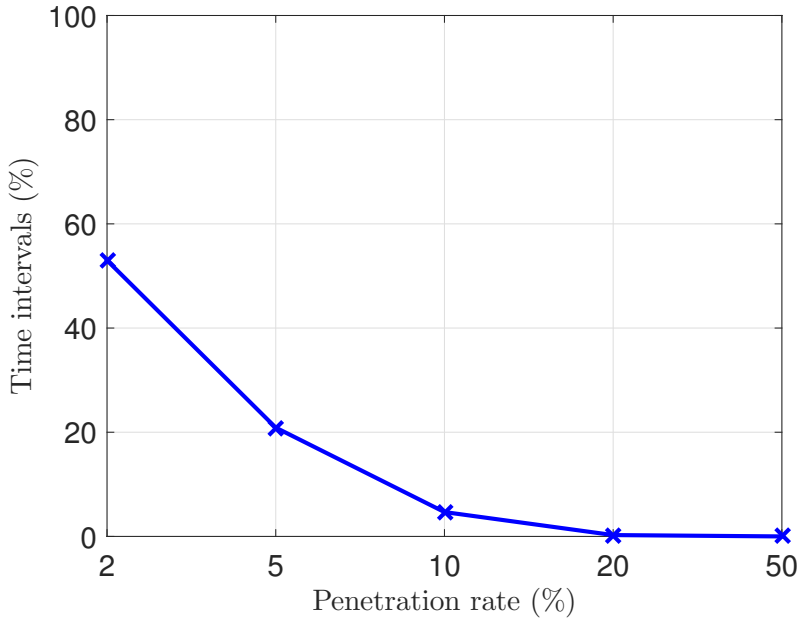


Fig. 6.1: Average percentage of time intervals of $T = 10$ s that feature no connected vehicle report against penetration rate of connected vehicles.

(i.e., when congested conditions are reported) overall speeds, whereas for medium speeds the difference is larger. The mean speed difference is almost zero at any speed. In addition, while the penetration rate of connected vehicles decreases, the SD of the error increases as shown in Fig. 6.3, while the mean error is almost zero for any penetration rate.

To address the problem of connected vehicle speed being non-representative of the average segment speed and the problem of having no connected vehicle reports in a segment for specific time intervals, the filter is fed with a moving average of the available speed measurements. More specifically, for every time step $k$, the filter is fed with a moving average of the $n$ latest measurements, i.e., with

$$\upsilon_i(k) = \sum_{j=0}^{n-1} \frac{\nu_i(k-j)}{n}, \tag{6.1}$$

where $\upsilon_i(k)$ is the speed that is utilized by the filter at time step $k$, and $\nu_i(k)$ is the average speed computed from connected vehicles reports at segment $i$ and time step $k$. Moreover, if there are no connected vehicle reports at all at segment $i$ during time interval $((k-1)T, kT]$, the speed $\nu_i(k)$ is chosen equal to the speed reported at the previous time step, i.e., $\nu_i(k) = \nu_i(k-1)$. Note that an alternative but more complex methodology for obtaining potentially more accurate measurements of the overall speed via connected vehicle reports is via application of traffic modelling as in Treiber et al. (2011), Rempe and Bogenberger (2016).

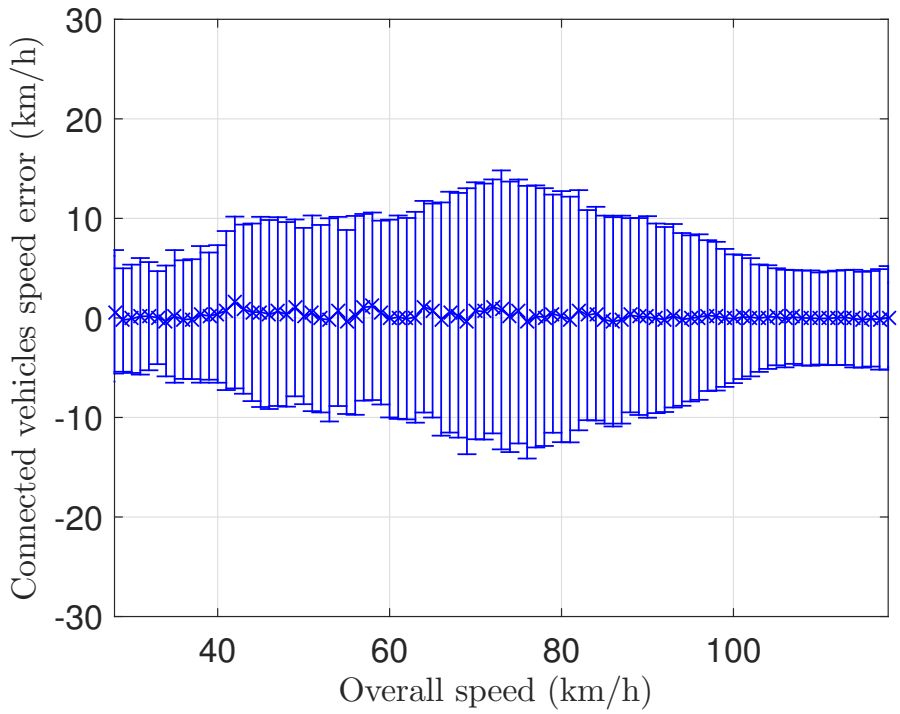


Fig. 6.2: Mean and SD of the error between actual segment speed and speed reported by connected vehicles, averaged over all segments and over 10 simulation replications, for a 20% penetration rate of connected vehicles.

A reasonable choice for $n$ in (6.1) is $n = 6$, since 60 s intervals are quite common for aggregation of data stemming from connected vehicles in literature, see, e.g., Rahmani et al. (2010), Lovisari et al. (2015). However, in our experiments, at very low penetration rates and light traffic, it is often the case that very few connected vehicles travel on a segment during 6 consecutive time intervals (i.e., 60 s). As a result, the filter may use speed measurements originating from very few (or even just one) connected vehicles, which may not be representative of the current segment speed. In order to tackle this issue, a larger time window for computing the average segment speeds from connected vehicle reports is also tested, employing (6.1) with $n = 12$. In fact, a complete absence of connected vehicle reports over the last 12 time intervals is very rare in our experiments.

Fig. 6.4 shows the mean and SD of the error between the actual segment speed and the speed that is utilized by the filter for both cases, i.e., when utilizing (6.1) with $n = 6$ and $n = 12$. It can be observed that for penetration rates lower than 10%, there is a small bias in the mean error that is similar for both cases, while the SD of the error is slightly smaller for $n = 12$. However, for penetration rates higher than 20%, there is no bias for either of the two cases, while the SD of the error is slightly smaller for $n = 6$. Consequently, for low penetration rates the average

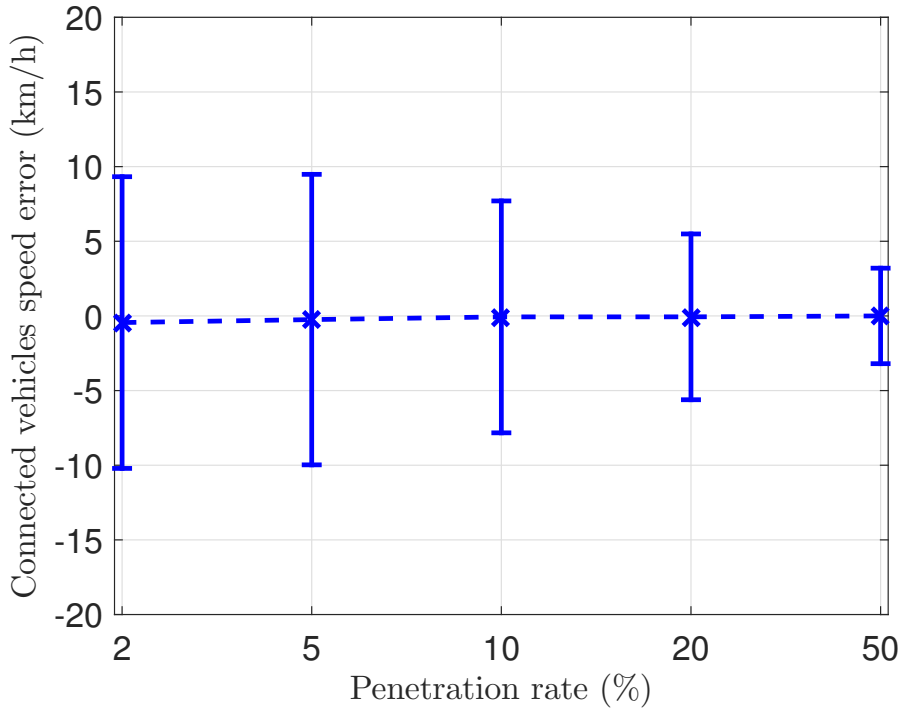


Fig. 6.3: Mean and SD of the error between actual segment speed and speed reported by connected vehicles, averaged over all segments, against penetration rate of connected vehicles.

speed, calculated via (6.1), is more representative of the overall segment speed for $n = 12$, whereas for higher penetration rates it is more representative for $n = 6$, albeit the corresponding differences are deemed minor.

## 6.3 Selection of the estimation scheme parameters

While employing the presented estimator in practice, it is important to minimize any necessary tuning effort for the involved parameters. This will certainly be the case if the estimator performance proves little sensitive to variations of these parameters within a broad range of values. To investigate this issue, a series of experiments are performed, evaluating the sensitivity of the estimation scheme to the values of the filter parameters $Q$ and $R$. To this end, the performance of the estimation is compared, when each of the involved parameters $\sigma_\rho$, $\sigma_{r,s}$, and $\sigma_R$ is varied by several orders of magnitude, while the other two remain constant. The results are shown in Fig. 6.5, for a variety of penetration rates of connected vehicles. It is evident in the plots that the performance of density estimation is highly insensitive to the values

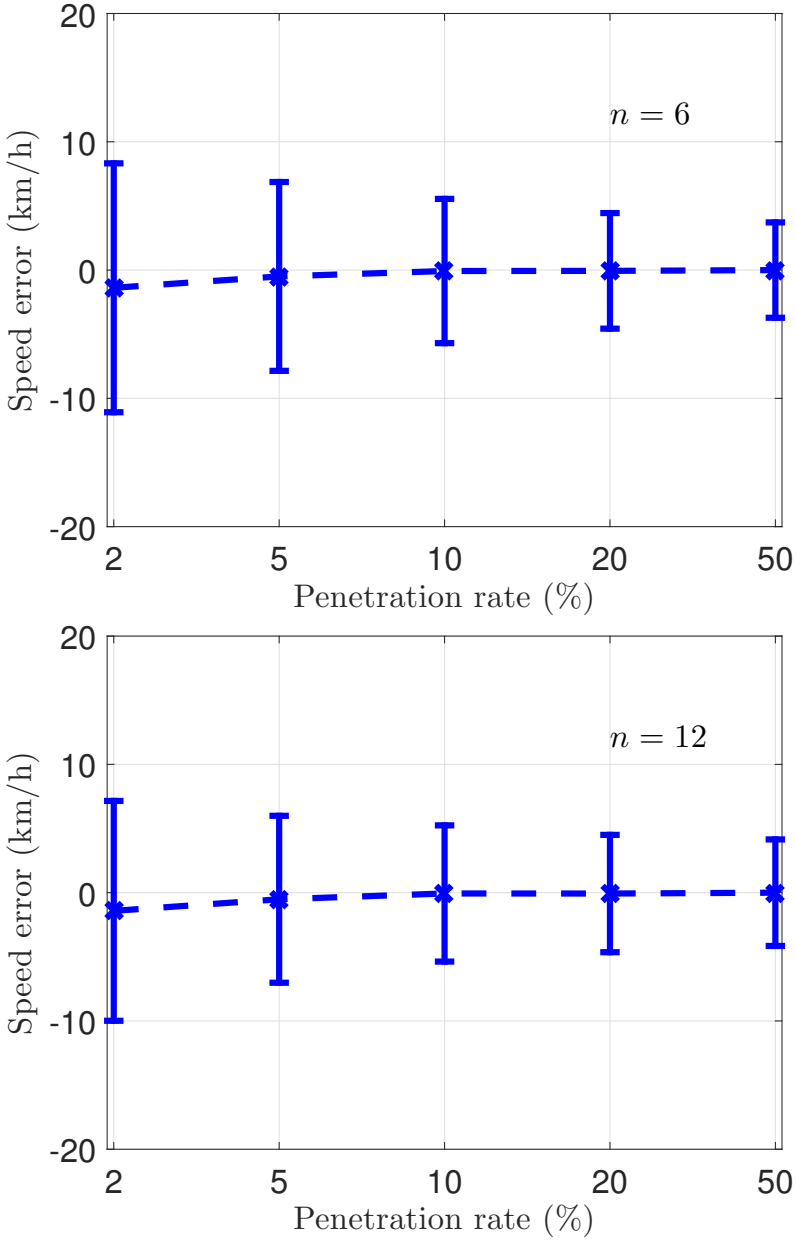


Fig. 6.4: Mean and SD of the error between actual segment speed and speed utilized by the estimation scheme averaged over all segments and over 10 simulation replications against penetration rate of connected vehicles when the speed utilized by the estimator is calculated via (6.1) for $n = 6$ (top) and $n = 12$ (bottom).

| $Q$ | $\sigma_\rho$ | $\sigma_{r,s}$ | $H$ |
|---|---|---|---|
| $\text{diag}(\sigma_\rho \times I_N, \sigma_{r,s} \times I_{(l_r+l_s)})$ | 1 | 0.03 | $I_{(N+l_r+l_s)}$ |
| $R$ | $\sigma_R$ | $\mu$ | |
| $\text{diag}(\sigma_R \times I_{(l_r+l_s)})$ | 100 | $(15, \ldots, 15, 5, \ldots, 5)^T$ | |

Table 6.1: Filter parameters used in the simulation in the case that all ramps are unmeasured.

of the filter parameters $\sigma_\rho$, $\sigma_{r,s}$, and $\sigma_R$. Ramp flow estimation is shown to be more sensitive, especially for low penetration rates of connected vehicles.

The same values as in the case of some ramps of the network being unmeasured described in Chapter 5 are chosen for the entry of matrix $Q$ that corresponds to densities and for matrix $R$ , while the entry of $Q$ that corresponds to unmeasured ramps is chosen as $\sigma_{r,s} \times I_{(l_r+l_s)}$, where $\sigma_{r,s}$ is equal to 0.03. Similarly, the initial values $\mu$ as well as matrix $H$ are chosen to be the same as in the case of fewer ramps being unmeasured; the values of the filter parameters are shown in Table 6.1. From Fig. 6.5 one can observe that this choice for the parameters $Q$ and $R$ results in quite low values for the performance indices for our basic scenario of 20% penetration rate of connected vehicles, as well as for all other investigated penetration rates, hence values of $Q$ and $R$ are kept the same throughout the rest of the text. However, for very low penetration rates, Fig. 6.5 may be exploited, if one desires to obtain a better ramp flow estimation performance (since density estimation is seen to be insensitive to the choice of $Q$ and $R$) by elaborating more on the choice of the parameters Q and R. In particular, according to Fig. 6.5, the simple rule that for low penetration rates the value of $\sigma_\rho$ needs to decrease, whereas the value of $\sigma_R$ needs to increase, may be considered.

## 6.4 Performance evaluation for varying penetration rates of connected vehicles

The results of the estimation of segment densities and ramp flows for a 20% penetration rate of connected vehicles are shown in Fig. 6.6 and Fig. 6.7, respectively, when the speed fed to the filter is calculated via (6.1) with $n = 6$. It is evident from the plots that the estimation is quite satisfactory, both for segment densities and for ramp flows. Segment density estimation is characterized by a performance index $CV_\rho = 17.4\%$, whereas ramp flow estimation is characterized by a performance

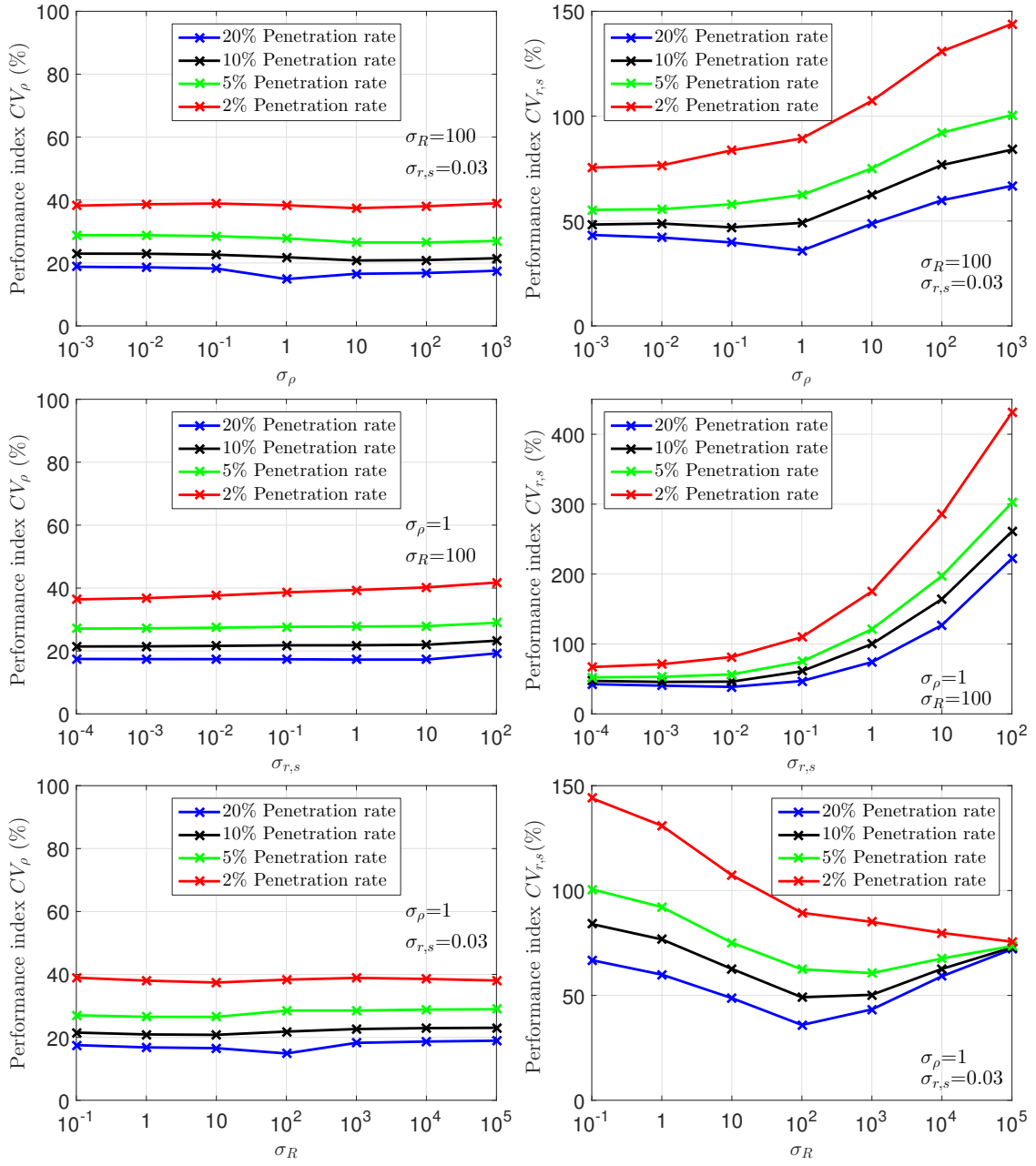


Fig. 6.5: Performance comparison of the density and ramp flow estimations for different values of the parameters $\sigma_\rho$ (top), $\sigma_{r,s}$ (middle), and $\sigma_R$ (bottom), for various penetration rates of connected vehicles, when the speed utilized by the estimator is calculated via (6.1) with $n = 6$.

index $CV_{r,s} = 39.0\%$. Fig. 6.8 and Fig. 6.9 show the results of density and ramp flow estimation for a 5% penetration rate of connected vehicles when the speed fed to the filter is calculated via (6.1) with $n = 6$. Density estimation is satisfactory, characterized by a performance index $CV_\rho = 27.8\%$, while ramp flow estimation is less satisfactory, characterized by a performance index $CV_{r,s} = 62.4\%$.

Fig. 6.10 and Fig. 6.11 show the results of density and ramp flow estimation for a 20% penetration rate of connected vehicles when the speed fed to the filter is calculated via (6.1) with $n = 12$. The estimation is quite satisfactory, both for segment densities and for ramp flows and is similar with the case of using (6.1) with $n = 6$, shown in Fig. 6.6 and Fig. 6.7. Segment density estimation is characterized by a performance index $CV_\rho = 16.6\%$, whereas ramp flow estimation is characterized by a performance index $CV_{r,s} = 37.4\%$. The results of the estimation for a 5% penetration rate of connected vehicles when the speed fed to the filter is calculated via (6.1) with $n = 12$ are shown in Fig. 6.12 and Fig. 6.13. Density estimation is characterized by a performance index $CV_\rho = 23.6\%$, while ramp flow estimation is characterized by a performance index $CV_{r,s} = 46.1\%$. Both the plots and the calculated performance indices indicate that using (6.1) with $n = 12$ results in a better estimation, especially for ramp flows.

The performance indices of the estimation when the speed utilized by the filter is calculated via (6.1) with $n = 6$ and with $n = 12$ are shown in Fig. 6.14, for varying penetration rates of connected vehicles. In the first case, the filter can estimate segment densities with a satisfactory performance even for penetration rates as low as 2%. For unmeasured ramp flows the results for penetration rates of 5% or lower are less satisfactory. In the second case, the utilization of the longer moving average improves the estimated segment densities as well as the unmeasured ramp flows, more evidently for penetration rates of 5% or lower. These results are in accordance with Fig. 6.4.

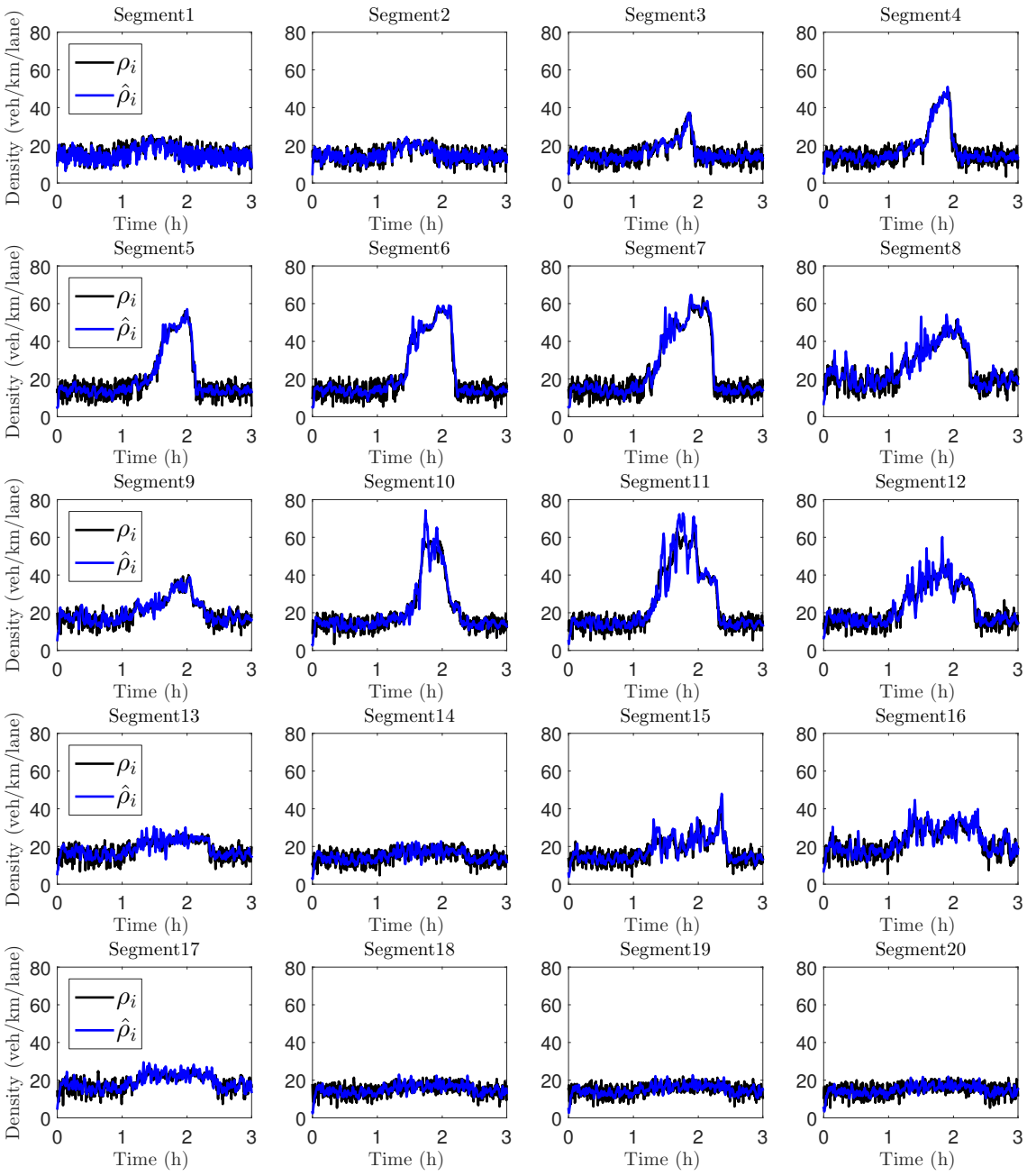


Fig. 6.6: Comparison between real (black line) and estimated (blue line) density per lane in veh/km for all network segments for mixed traffic with a 20% penetration rate of connected vehicles when the speed fed to the filter is calculated via (6.1) with $n = 6$.

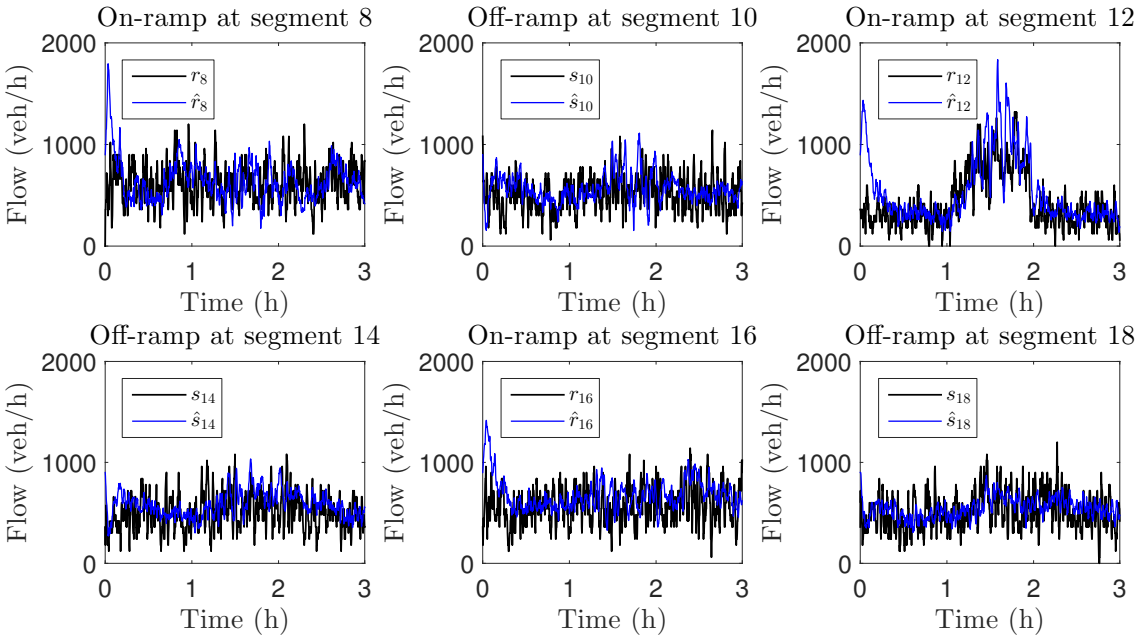


Fig. 6.7: Comparison between real (black line) and estimated (blue line) ramp flow in veh/h for all network on-ramps and off-ramps for mixed traffic with a 20% penetration rate of connected vehicles when the speed fed to the filter is calculated via (6.1) with $n = 6$.

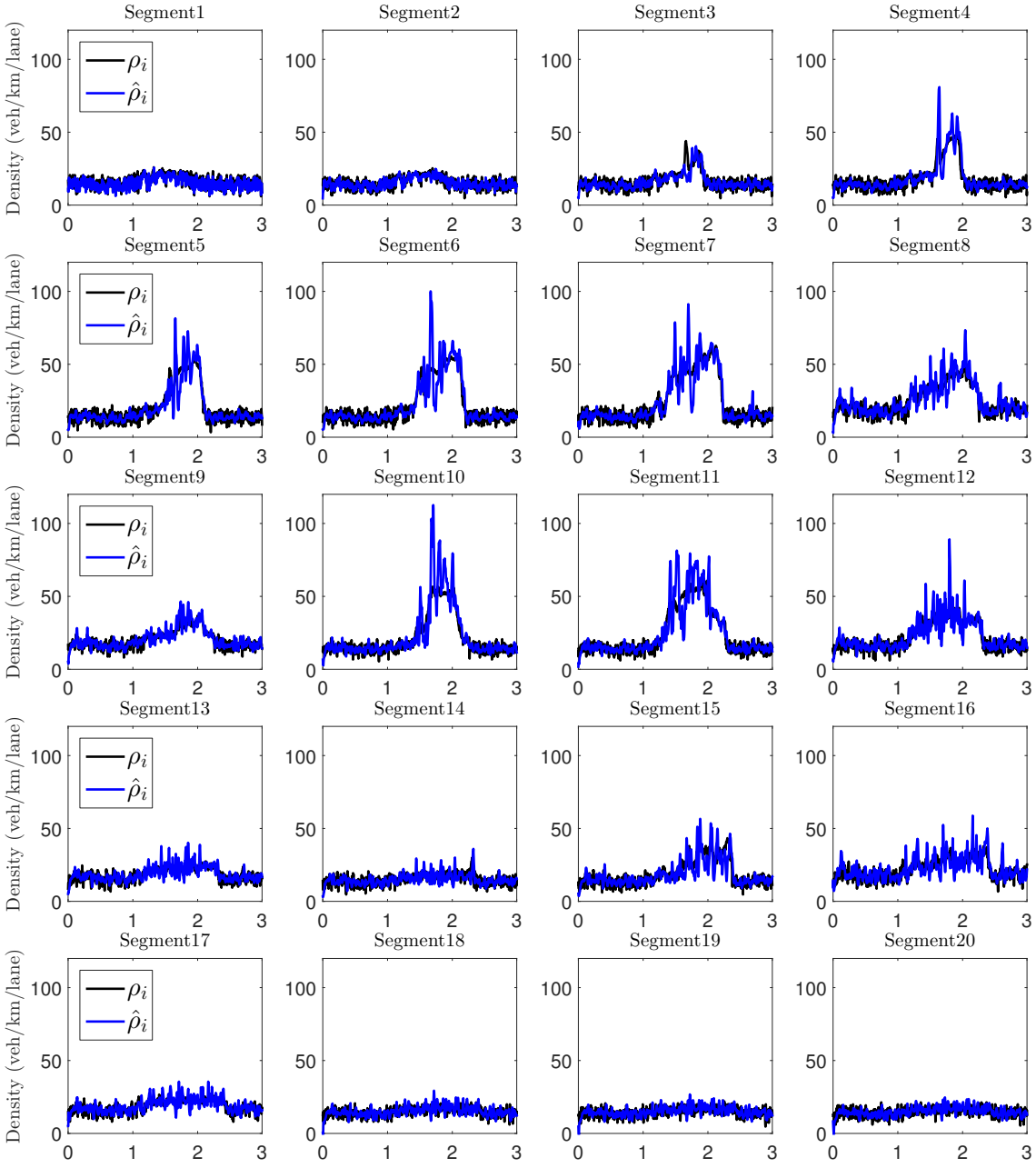


Fig. 6.8: Comparison between real (black line) and estimated (blue line) density per lane in veh/km for all network segments for mixed traffic with a 5% penetration rate of connected vehicles when the speed fed to the filter is calculated via (6.1) with $n = 6$.

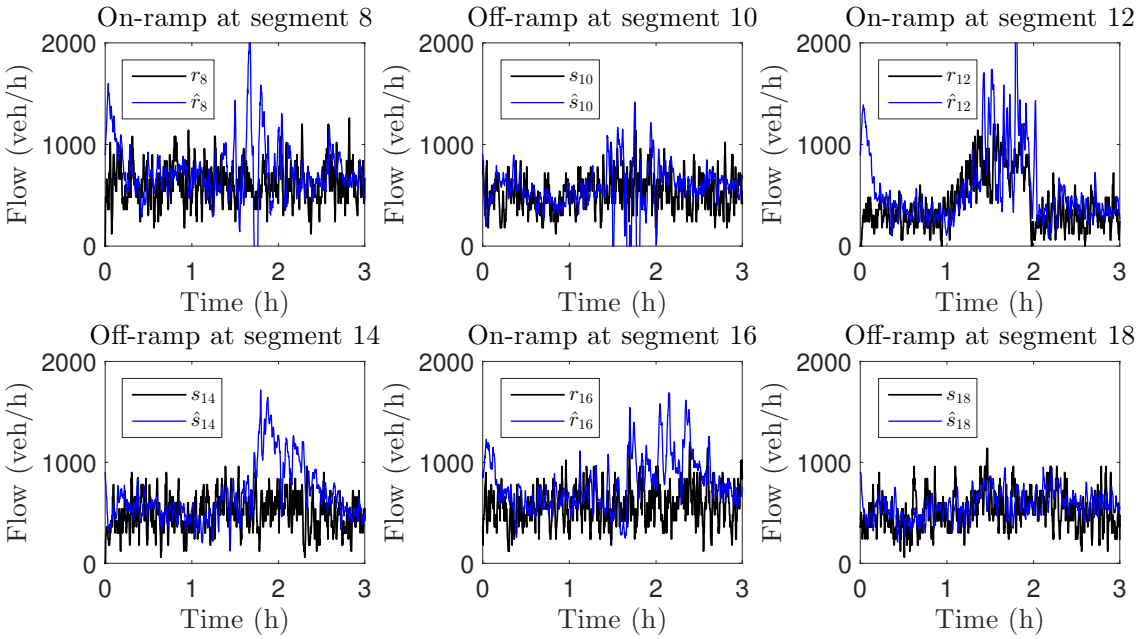


Fig. 6.9: Comparison between real (black line) and estimated (blue line) ramp flow in veh/h for all network on-ramps and off-ramps for mixed traffic with a 5% penetration rate of connected vehicles when the speed fed to the filter is calculated via (6.1) with $n = 6$.

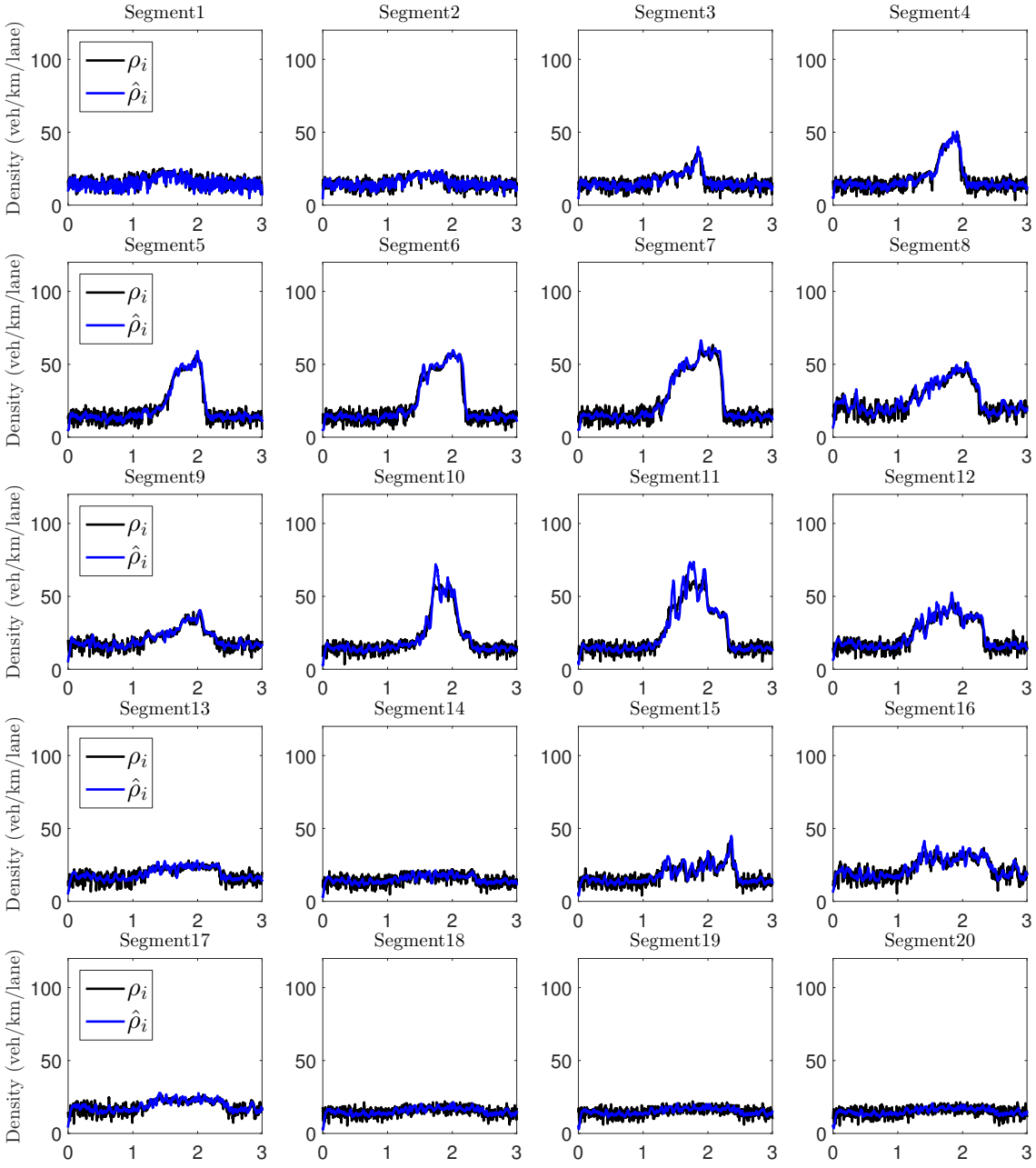


Fig. 6.10: Comparison between real (black line) and estimated (blue line) density per lane in veh/km for all network segments for mixed traffic with a 20% penetration rate of connected vehicles when the speed fed to the filter is calculated via (6.1) with $n = 12$.

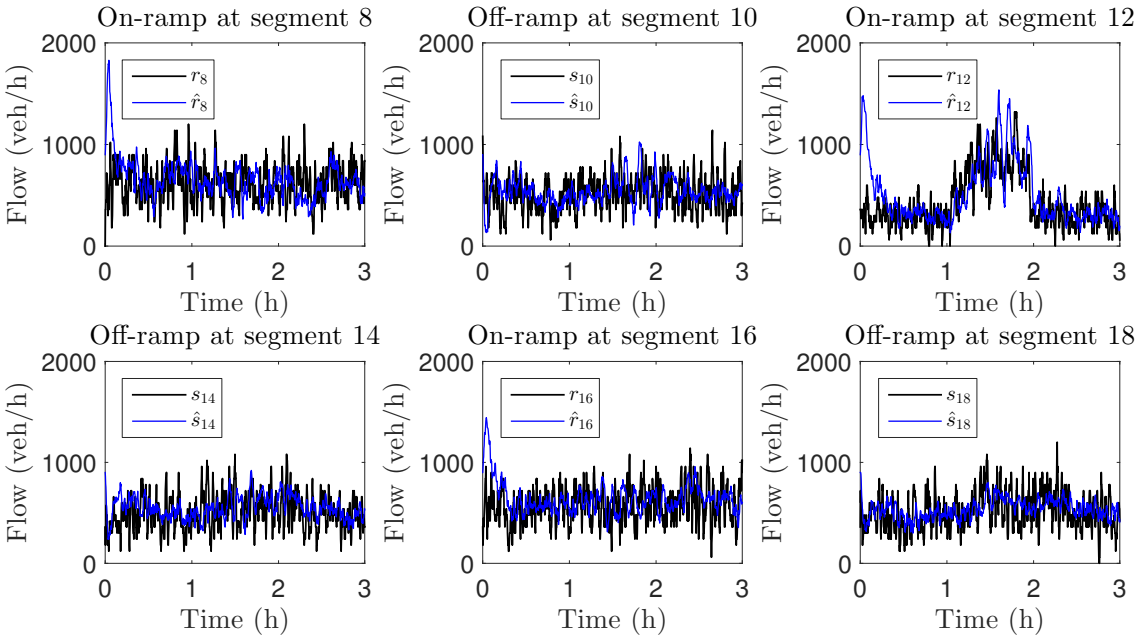


Fig. 6.11: Comparison between real (black line) and estimated (blue line) ramp flow in veh/h for all network on-ramps and off-ramps for mixed traffic with a 20% penetration rate of connected vehicles when the speed fed to the filter is calculated via (6.1) with $n = 12$.

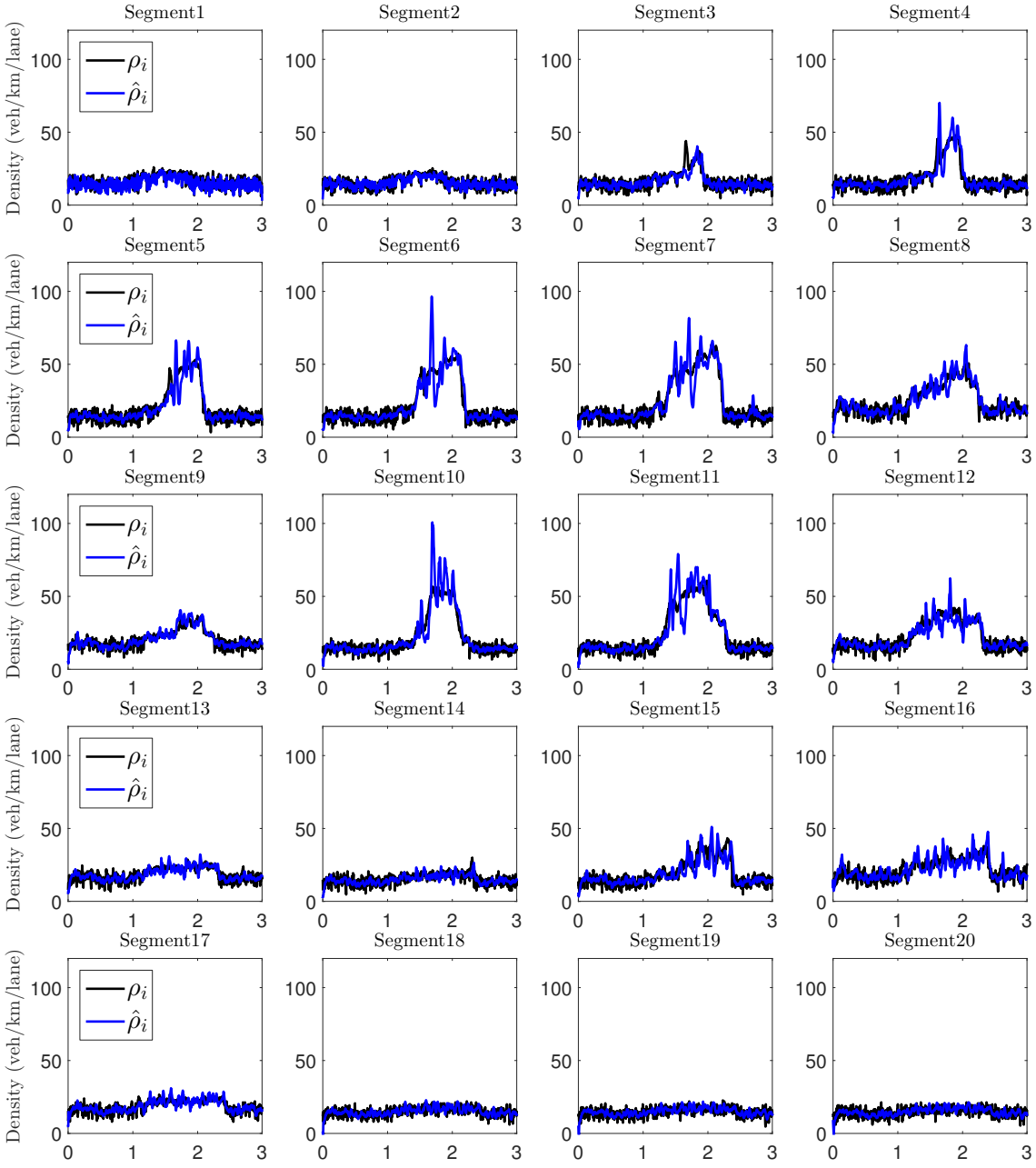


Fig. 6.12: Comparison between real (black line) and estimated (blue line) density per lane in veh/km for all network segments for mixed traffic with a 5% penetration rate of connected vehicles when the speed fed to the filter is calculated via (6.1) with $n = 12$

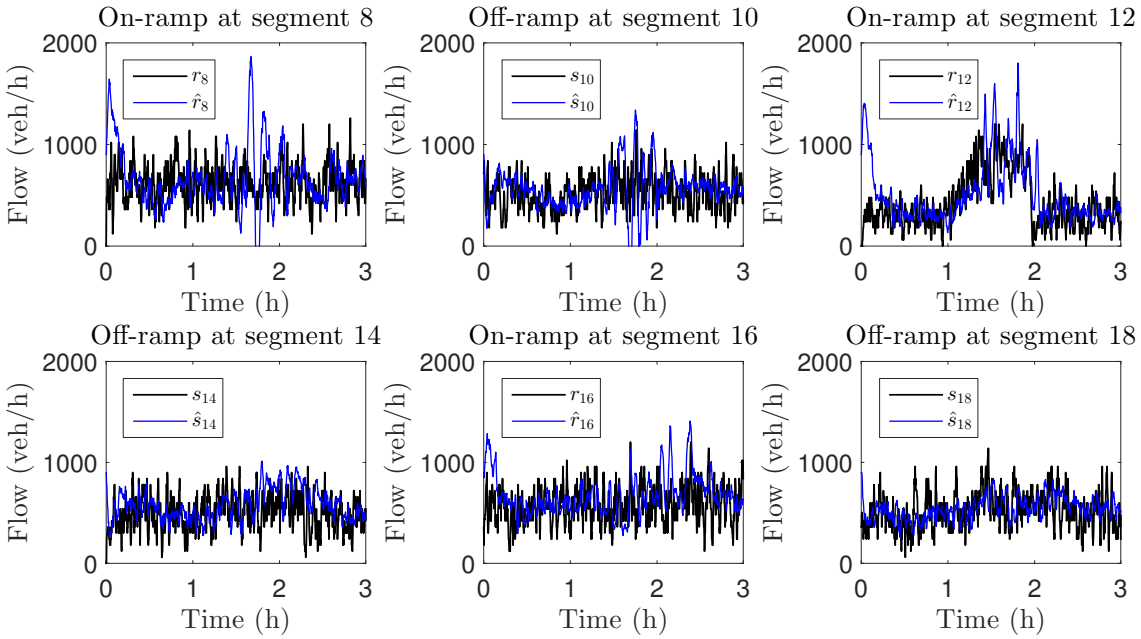


Fig. 6.13: Comparison between real (black line) and estimated (blue line) ramp flow in veh/h for all network on-ramps and off-ramps for mixed traffic with a 5% penetration rate of connected vehicles when the speed fed to the filter is calculated via (6.1) with $n = 12$

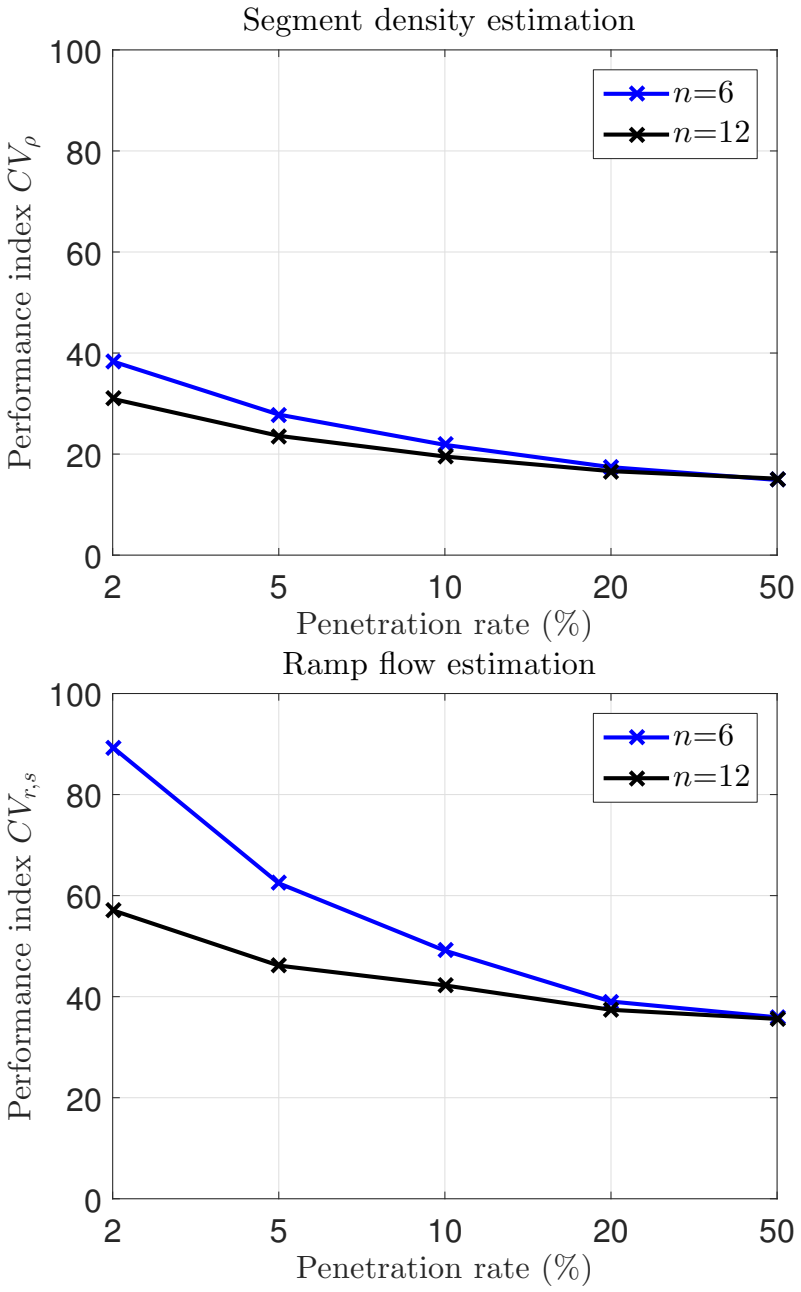


Fig. 6.14: Performance indices of density estimation $CV_\rho$ (top) calculated via (4.1) and ramp flow estimation $CV_{r,s}$ (bottom) calculated via (5.3) for varying penetration rates of connected vehicles when the speed fed to the filter is calculated via (6.1).

# Chapter 7

# Mixed traffic estimation results in the presence of regular and ACC-equipped vehicles

## 7.1 Model of the ACC-equipped vehicles

In this section, in order to further evaluate the performance of the proposed estimation scheme under more heterogeneous conditions, a scenario of mixed traffic comprising conventional vehicles and connected vehicles equipped with an ACC system is considered. ACC-equipped connected vehicles can communicate data to the central authority concerning their state, but feature a different car-following behavior than conventional vehicles. Thus, the performance of our estimation scheme is evaluated not only when data, gathered from the central authority, stem from a small fraction of the total vehicle population, but also when these connected vehicles behave differently than conventional vehicles.

For our experiments, ACC-equipped vehicles are characterized by a different car-following model than the one used for conventional vehicles. While the default car-following model implemented in Aimsun is the Gipps model (Gipps, 1981, 1986), the following Constant Time-Gap (CTG) model is considered for an ACC-equipped vehicle $i$, used in Rajamani et al. (2005), similar to the one proposed by Liang and Peng (1999),

$$\ddot{x}_i = K_1(x_{i-1} - x_i - L_{i-1} - h_d\dot{x}_i) + K_2(\dot{x}_{i-1} - \dot{x}_i), \tag{7.1}$$

where index $i-1$ refers to the vehicle preceding vehicle $i$; $x_i$, $\dot{x}_i$, and $\ddot{x}_i$ are the position, speed, and acceleration of vehicle $i$, respectively; $L_i$ is the length of vehicle $i$; $h_d$ is the desired time-headway; and $K_1$, $K_2$ are control gains. Moreover, the

acceleration $\ddot{x}$ is restricted between $d_i$ and $\alpha_i$, which are the maximum deceleration and acceleration of vehicle $i$, respectively. In addition, when the speed of vehicle $i$ computed based on (7.1) surpasses a certain treshold, say $V_i^*$, then it is set equal to this maximum speed. The values for the parameters of the model described by (7.1) are given in the next section.

## 7.2 Experimental configuration

The scenario described in Section 5 is considered in this section. The control gains are set at the values proposed by Liang and Peng (1999), namely $K_1 = 1.12$ and $K_2 = 1.70$. Moreover, the time headway $h_d$ is chosen in the lower side of the typical range (Kesting et al., 2007), randomly set for each ACC vehicle, according to a bounded, between 0.5 and 2 s, normal distribution with a mean of 0.8 s and an SD of 0.2 s. Finally, the simulation step is set equal to 0.2 s.

Since ACC-equipped vehicles feature a different behavior than conventional vehicles and, as mentioned in Section 1, a substantial percentage of ACC-equipped vehicles affects directly the traffic dynamics, different traffic conditions are expected in a scenario with mixed traffic comprising conventional and ACC-equipped vehicles than in the case of conventional and connected vehicles discussed in Section 6. As in the connected vehicles case, the performance of the estimation scheme is evaluated for a variety of penetration rates of ACC-equipped vehicles and 10 simulation replications are considered for each penetration rate. Fig. 7.1 shows the traffic conditions created for a 20% penetration rate of ACC-equipped vehicles. Comparing Fig. 7.1 with Fig. 4.1, one can see that, due to the presence of ACC-equipped vehicles, congestion is milder than with conventional vehicles only. In this case, congestion is created during the second hour of the simulation, at segments 12 and 8, where the first two on-ramps are located, and propagates upstream reaching segment 6. At the location of the third on-ramp, i.e., at segment 16, some reduction of speed is observed, but without a severe congestion being evident. Halfway through the third hour of the simulation, after the inflows at the network entry and at on-ramp 12 are decreased, free flow conditions are restored until the end of the simulation time.

## 7.3 Computation of the measurements utilized by the estimator

As explained in Section 6.2, the developed estimation scheme is based on the assumption that the average connected vehicles speed roughly equals the average con-

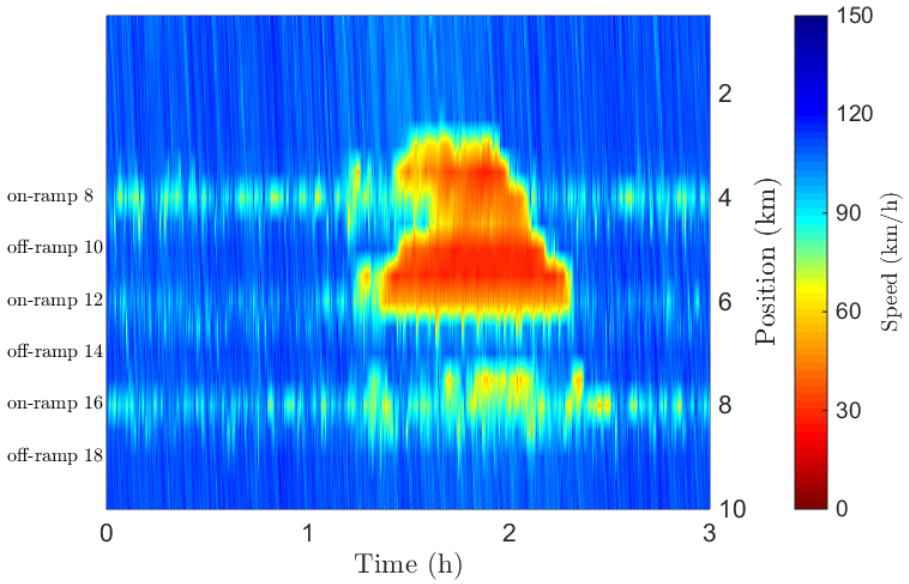


Fig. 7.1: Average speed of all vehicles in the employed simulation scenario of mixed traffic comprising conventional and ACC-equipped vehicles, for a 20% penetration rate of ACC-equipped vehicles.

ventional vehicles speed. However, since the behavior of ACC-equipped vehicles differs from the behavior of conventional vehicles, the accuracy of this assumption needs to be re-examined for the case of mixed traffic comprising ACC-equipped and conventional vehicles. Similar issues as in the case of regular connected vehicles described in Section 6.2, appear also when calculating the average segment speed from reports of ACC-equipped vehicles. Besides the problem of no ACC-equipped vehicle being present in a segment during a time interval of $T = 10$ s in cases of low penetration rates, the different behavior between the two types of vehicles also increases the inaccuracy in the computation of the average segment speed. Fig. 7.2 shows the percentage of time intervals of $T = 10$ s that feature no ACC-equipped vehicle report, averaged over all segments and replications. The results are very similar with the conventional connected vehicles case, showing that for penetration rates of 10% or lower a substantial percentage of time intervals are bare of reports from ACC-equipped vehicles.

Moreover, Fig. 7.3 presents the speed error between ACC-equipped vehicles speed and overall speed for a 20% penetration rate of ACC-equipped vehicles. One can observe that there is a bias in the speed of ACC-equipped vehicles in comparison to the actual speed, which is less prominent at high or low speeds. Speeds that are considered "medium" typically correspond to traffic conditions that appear during transitions between congested and free-flow traffic, i.e., time intervals when

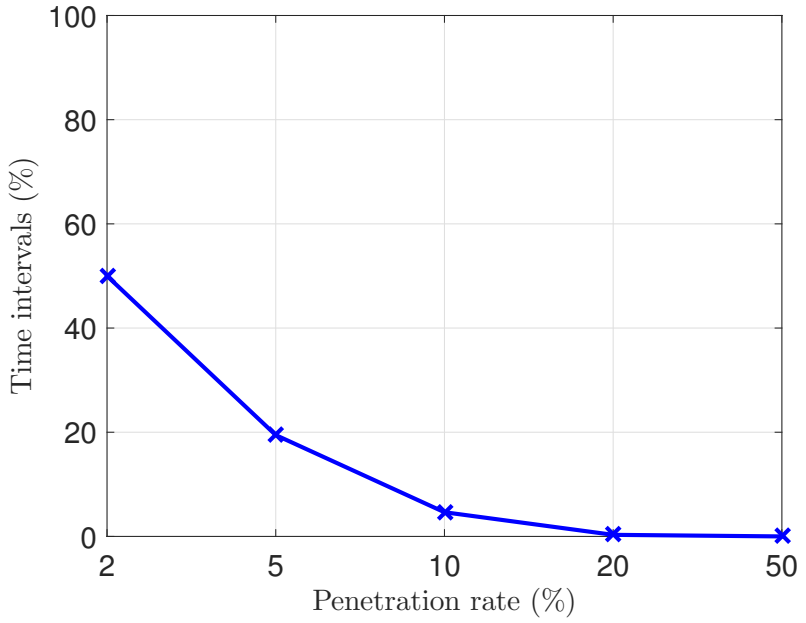


Fig. 7.2: Average percentage of time intervals of $T = 10$ s that feature no ACC-equipped vehicle report against penetration rate of ACC-equipped vehicles.

congestion is forming or dissolving. When congestion is forming, vehicles decelerate to match the preceding vehicles' speed, and thus, the low time-headway of ACC-equipped vehicles allows them to avoid excessive breaking which in turn enables them to hold a higher average speed. When congestion is dissolving vehicles typically accelerate aiming to reach their free-flow speed. In that case ACC-equipped vehicles are able to match the preceding vehicle's speed faster, thus holding a higher average speed. Detailed microscopic simulation comparison between the acceleration behavior of ACC-equipped and regular vehicles are reported by Rajamani et al. (2005).

Moreover, for a small interval of actual speed between $45-50$ km/h, which mainly corresponds to when vehicles are entering congestion, the bias is close to zero. After close examination of the traffic conditions when this speed range mostly appears, it is observed that the majority of speed samples are collected during phases that congestion is forming and the traffic is not homogenous because congestion is created due to the high inflows at on-ramps. As a result, the rightmost lane becomes congested whereas in the leftmost lane much higher speeds prevail, two speed categories in which the ACC-equipped vehicles generally exhibit a similar speed to regular vehicles. This way, although the average segment speed is considered as "medium", vehicles exhibit behavior that is characteristic to different traffic conditions.

Fig. 7.4 shows the mean and SD of the speed error between actual speed and

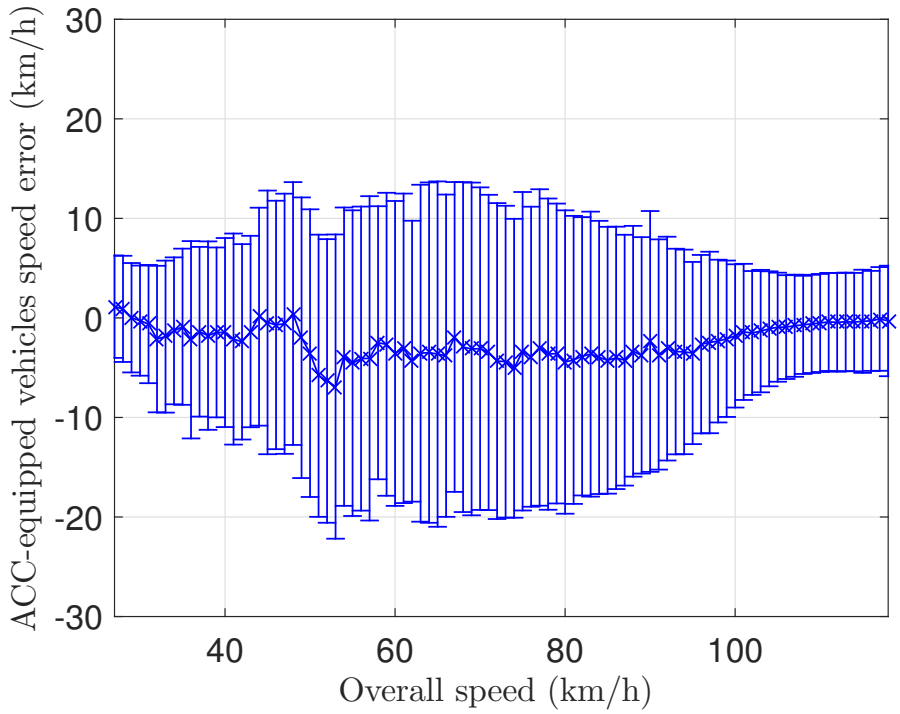


Fig. 7.3: Mean and SD of the error between actual segment speed and speed reported by ACC-equipped vehicles, averaged over all segments and over 10 simulation replications, for a 20% penetration rate of ACC-equipped vehicles.

speed reported by ACC-equipped vehicles for various penetration rates of ACC-equipped vehicles. It is evident that both the bias and SD of the error are increasing as the penetration rate is decreasing. Compared to Fig. 6.3 one can observe that larger SD and bias are evident in the case of ACC-equipped connected vehicles, which are further grown as the penetration rate is decreasing, since at low penetration rates the effect of ACC-equipped vehicles on traffic is smaller.

Since, as shown in Fig. 7.2, Fig. 7.3, and Fig. 7.4, it is possible that the speed gathered from ACC-equipped vehicles may be non-representative of the overall segment speed, or there may be no ACC-vehicle reports for some time steps, (6.1) needs to be employed for computing the speed that is utilized by the estimator. Fig. 7.5 shows the mean and SD of the error between the actual segment speed (all vehicles) and the speed that is utilized by feed the filter for the case of mixed traffic featuring conventional and ACC-equipped vehicles when utilizing (6.1) with $n = 6$ and $n = 12$. It is evident in the plots that for penetration rates lower than 10% there is a bias in the mean error that is similar for both cases, while the SD of the error is smaller for $n = 12$. For penetration rates higher than 20%, there is a smaller bias for both cases, while the SD of the error is slightly smaller for $n = 6$. The results exhibit a similar pattern with the conventional connected vehicles case,

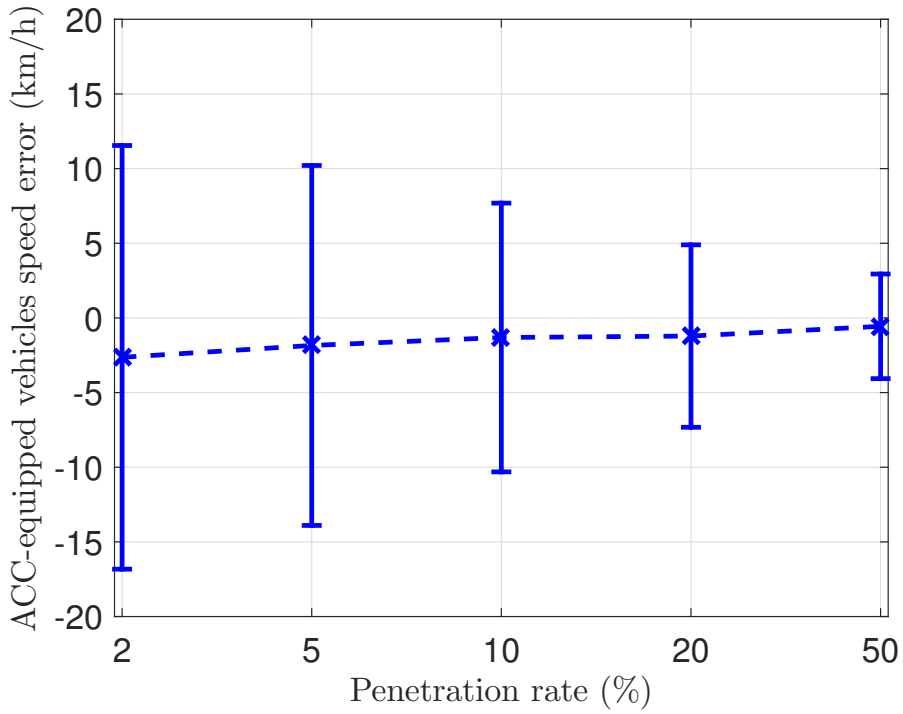


Fig. 7.4: Mean and SD of the error of between actual segment speed and speed reported by ACC-equipped vehicles, averaged over all segments, against penetration rate of ACC-equipped vehicles.

however, both the bias and SD of the error are larger in the ACC-equipped vehicles case, indicating that the speed that is utilized by the filter is less representative of the overall segment speed than in the connected vehicles case.

## 7.4 Performance evaluation for varying penetration rates of ACC-equipped vehicles

The same values for the filter parameters as in the case of regular connected vehicles, which are shown in Table 6.1, are considered in this case. The results of segment densities estimation for a penetration rate of 20% of ACC-equipped connected vehicles when the speed fed to the filter is calculated via (6.1) with $n = 6$ are shown in Fig. 7.6, while results of ramp flows estimation are shown in Fig. 7.7. The estimation results appear accurate for segment densities as well as for ramp flows, with resulting performance indices equal to $CV_\rho = 19.6\%$ and $CV_{r,s} = 45.3\%$, respectively. Fig. 7.8 and Fig. 7.9 show the results of density and ramp flow estimation for a 5% penetration rate of ACC-equipped vehicles when the speed fed to the filter is calculated via (6.1) with $n = 6$. Density estimation is fair, characterized by a

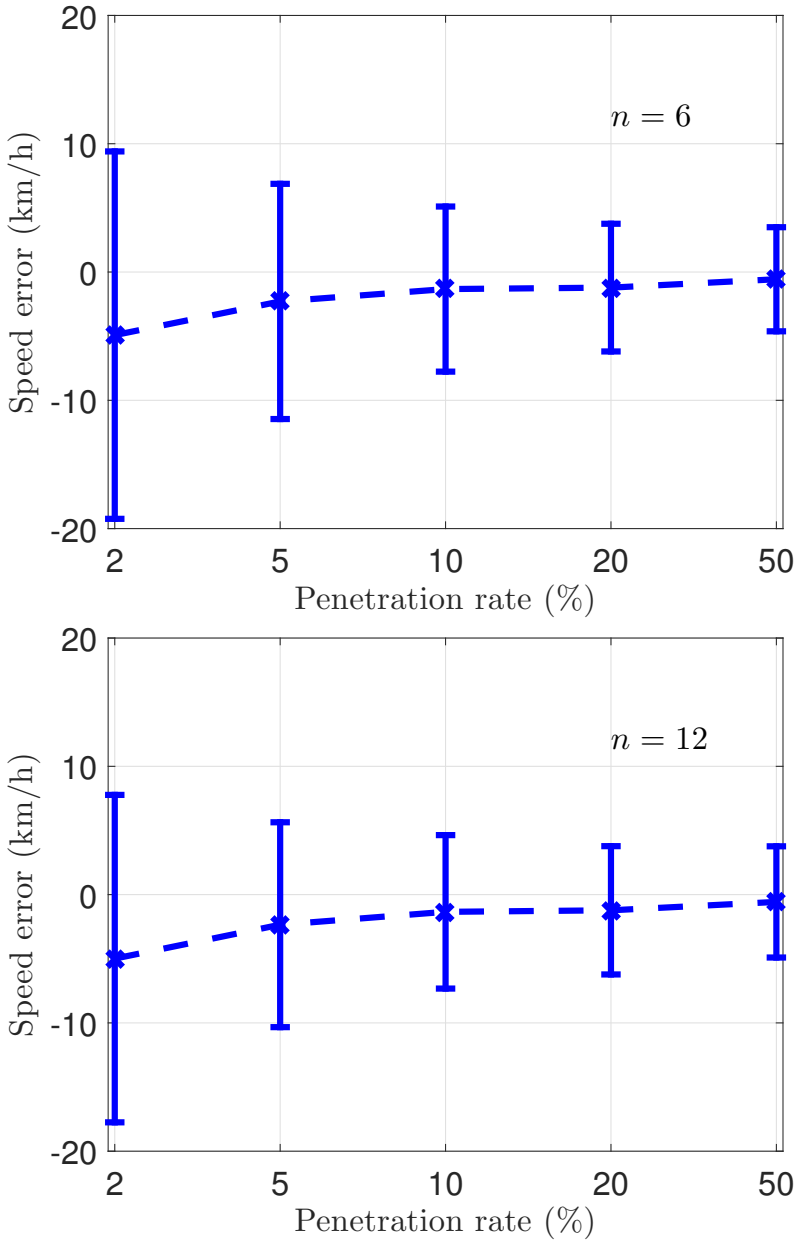


Fig. 7.5: Mean and SD of the error between actual segment speed (all vehicles) and speed utilized by the estimation scheme averaged over all segments and over 10 simulation replications against penetration rate of ACC-equipped vehicles when the speed utilized by the estimator is calculated via (6.1) for $n = 6$ (top) and $n = 12$ (bottom).

performance index $CV_\rho = 48.3\%$, while ramp flow estimation is not satisfactory, characterized by a performance index $CV_{r,s} = 183.7\%$.

Fig. 7.10 and Fig. 7.11 show the results of densities and ramp flows estimation for a 20% penetration rate of ACC-equipped vehicles when the speed fed to the filter is calculated via (6.1) with $n = 12$. The estimation results appear accurate for segment densities as well as ramp flows, showing a slight improvement from the case of $n = 6$, with resulting performance indices equal to $CV_\rho = 19.1\%$ and $CV_{r,s} = 42.3\%$, respectively. The results of the estimation for a 5% penetration rate of ACC-equipped vehicles when the speed fed to the filter is calculated via (6.1) with $n = 12$ are shown in Fig. 7.12 and Fig. 7.13. Density estimation is satisfactory, characterized by a performance index $CV_\rho = 33.0\%$, while ramp flow estimation is fair, characterized by a performance index $CV_{r,s} = 71.4\%$. Both the plots and the calculated performance indices indicate that using (6.1) with $n = 12$ results in a much better estimation, especially for ramp flows and low penetration rates. Performance indices of the estimation when using (6.1) with $n = 12$ for various penetration rates of ACC-equipped vehicles are shown in Fig. 7.14. The results of density estimation are quite satisfactory for penetration rates of 5% or higher, and fair for lower penetration rates. The results of ramp flow estimation are satisfactory for penetration rates higher than 5%, and only fair for penetration rates of 5% or lower.

## 7.5 Performance evaluation for varying penetration rates of ACC-equipped vehicles with a look-ahead speed feature

In this section, the performance of the proposed estimation scheme in the case of mixed traffic comprising conventional and ACC-equipped vehicles is tested, when ACC-equipped vehicles report to the central authority the speed of the preceding vehicle besides their own. As mentioned in Section 2.1, ACC-equipped vehicles are capable of acquiring the speed and position of the preceding vehicle (in order to regulate their own speed and position) via on-board sensors, which feature a range of up to 200 m (Abou-Jaoude, 2003).

In order to extend the information stemming from ACC-equipped vehicles, a system in which, whenever an ACC-equipped vehicle reports its location and speed to the central authority, it also reports the speed of the preceding vehicle, if the distance of the latter is lower than 200 m, is implemented. Furthermore, this addi-

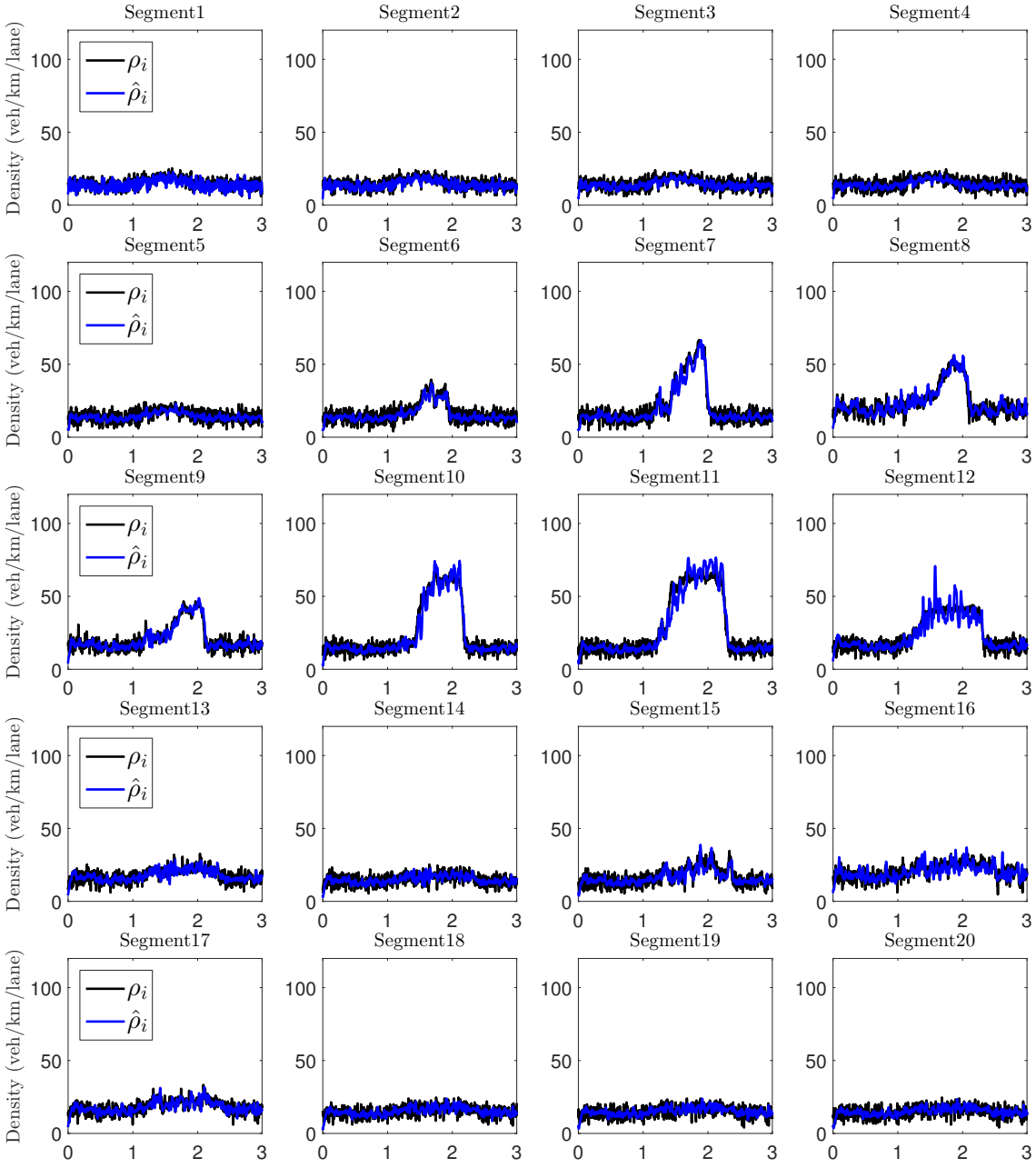


Fig. 7.6: Comparison between real (black line) and estimated (blue line) density per lane in veh/km for all network segments for mixed traffic with a 20% penetration rate of ACC-equipped vehicles when the speed fed to the filter is calculated via (6.1) with $n = 6$.

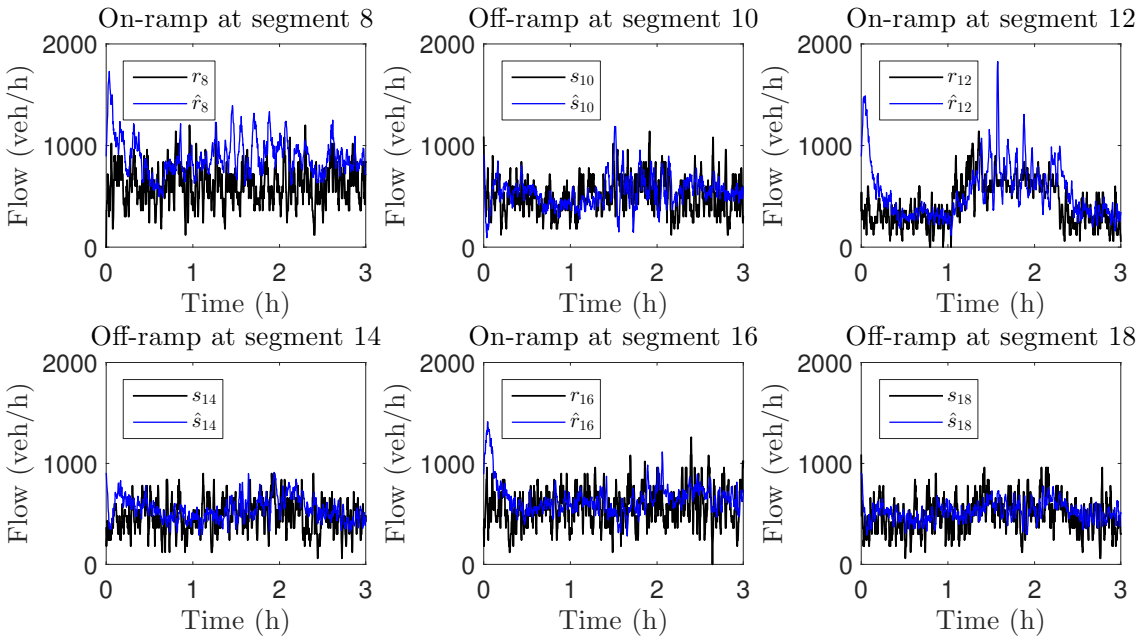


Fig. 7.7: Comparison between real (black line) and estimated (blue line) ramp flow in veh/h for all network on-ramps and off-ramps for mixed traffic with a 20% penetration rate of ACC-equipped vehicles when the speed fed to the filter is calculated via (6.1) with $n = 6$.

tional reporting happens only if the preceding vehicle is not reporting its own speed at the same time, so that the speed information of an individual vehicle is not used twice at the same reporting instant; in reality, this may be achieved by the central authority, which can identify the duplicate information from the two vehicles by matching their position and discard the unnecessary report. Consequently, when an ACC-equipped vehicle is reporting its speed, if its preceding vehicle, within a distance of 200 m, is not reporting its speed at this time, the preceding vehicle's speed is also taken into account when calculating the segment speed as if it was reporting itself.

The traffic network and scenario used in Section 7.4 are considered and 10 replications are simulated, for each penetration rate, when ACC-equipped vehicles feature enhanced speed reports. Fig. 7.15 compares the performance of the estimation when ACC-equipped vehicles feature enhanced reports to the performance of the estimation when ACC-equipped vehicles feature normal reports. In both cases, the average segment speed is computed using (6.1) with $n = 12$. It is evident in the plots that the estimation performance, both in terms of segment densities and ramp flows, is virtually identical for both cases.

This can be explained as follows. In spite of the fact that the look-ahead feature

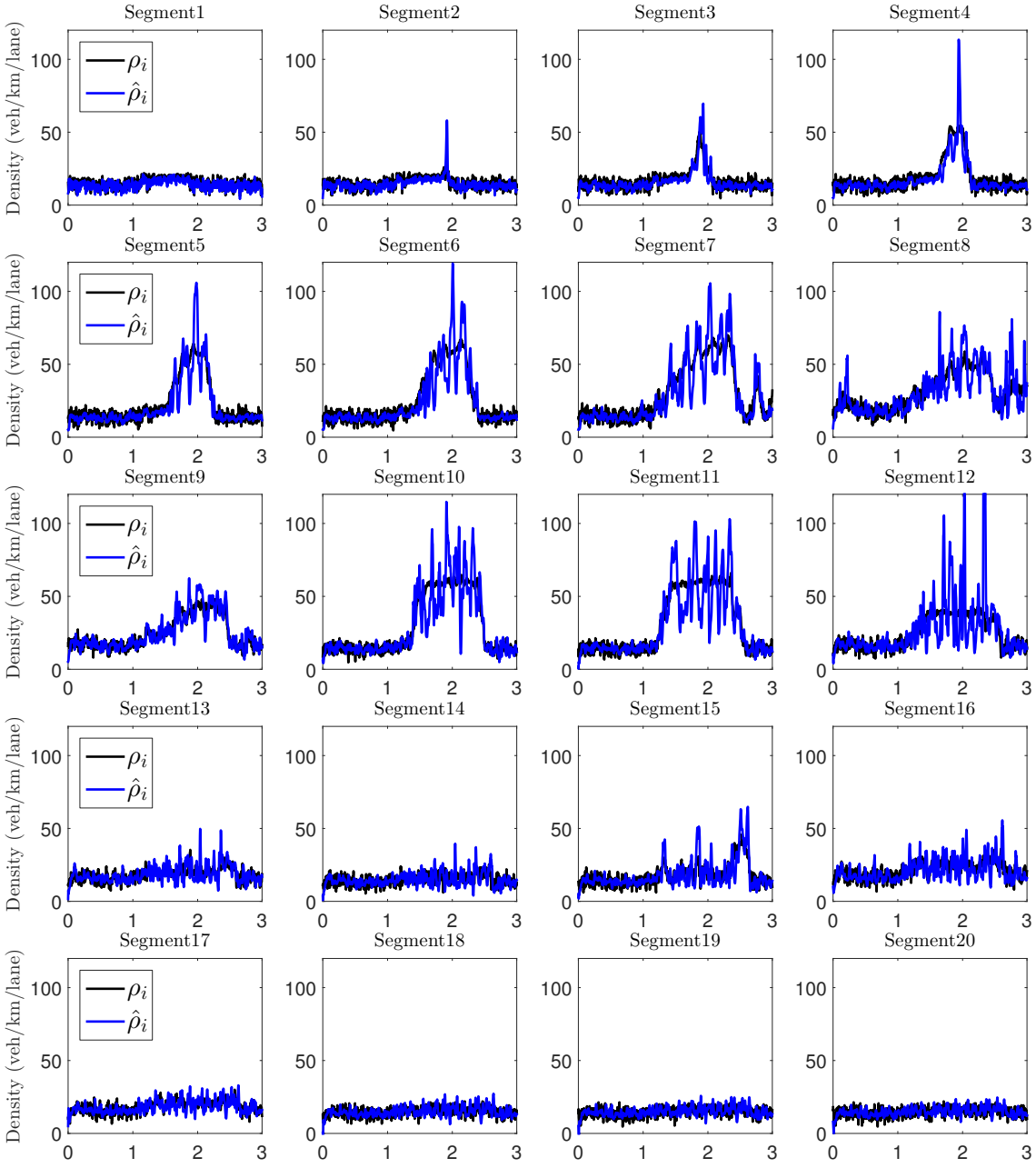


Fig. 7.8: Comparison between real (black line) and estimated (blue line) density per lane in veh/km for all network segments for mixed traffic with a 5% penetration rate of ACC-equipped vehicles when the speed fed to the filter is calculated via (6.1) with $n = 6$.

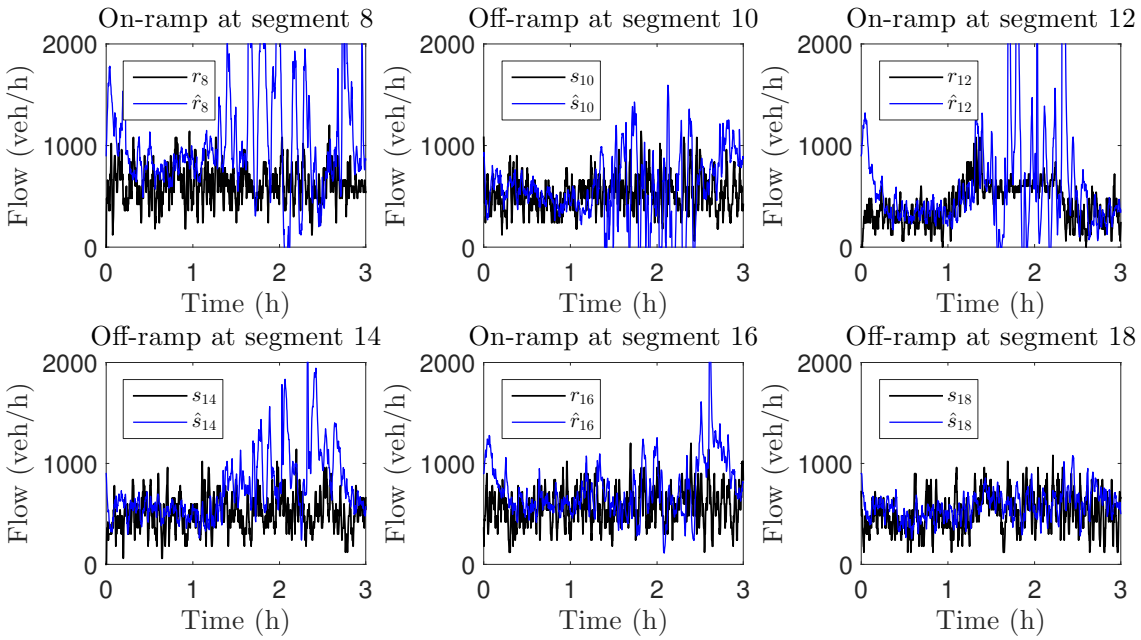


Fig. 7.9: Comparison between real (black line) and estimated (blue line) ramp flow in veh/h for all network on-ramps and off-ramps for mixed traffic with a 5% penetration rate of ACC-equipped vehicles when the speed fed to the filter is calculated via (6.1) with $n = 6$.

in most cases provides an additional vehicle speed measurement, thus doubling the available information, it has been observed in the simulations that the speed of the preceding vehicle is typically very similar to the ACC-equipped vehicle's speed. The ACC system is designed to be able to track the speed of the preceding vehicle, maintaining a specific time gap between the two vehicles. Especially in low time-gap configurations, as is our case, ACC-equipped vehicles manage to accurately follow the preceding vehicle's speed, except for very few occasions. This way, although double reports are obtained, the information is, in fact, almost identical, hence it fails to improve the estimation performance. Moreover, in cases where there are no ACC-equipped vehicles passing through a segment for a specific time interval, the problem of the lack of information remains regardless of the look-ahead feature, and thus, there is no improvement in the estimation performance.

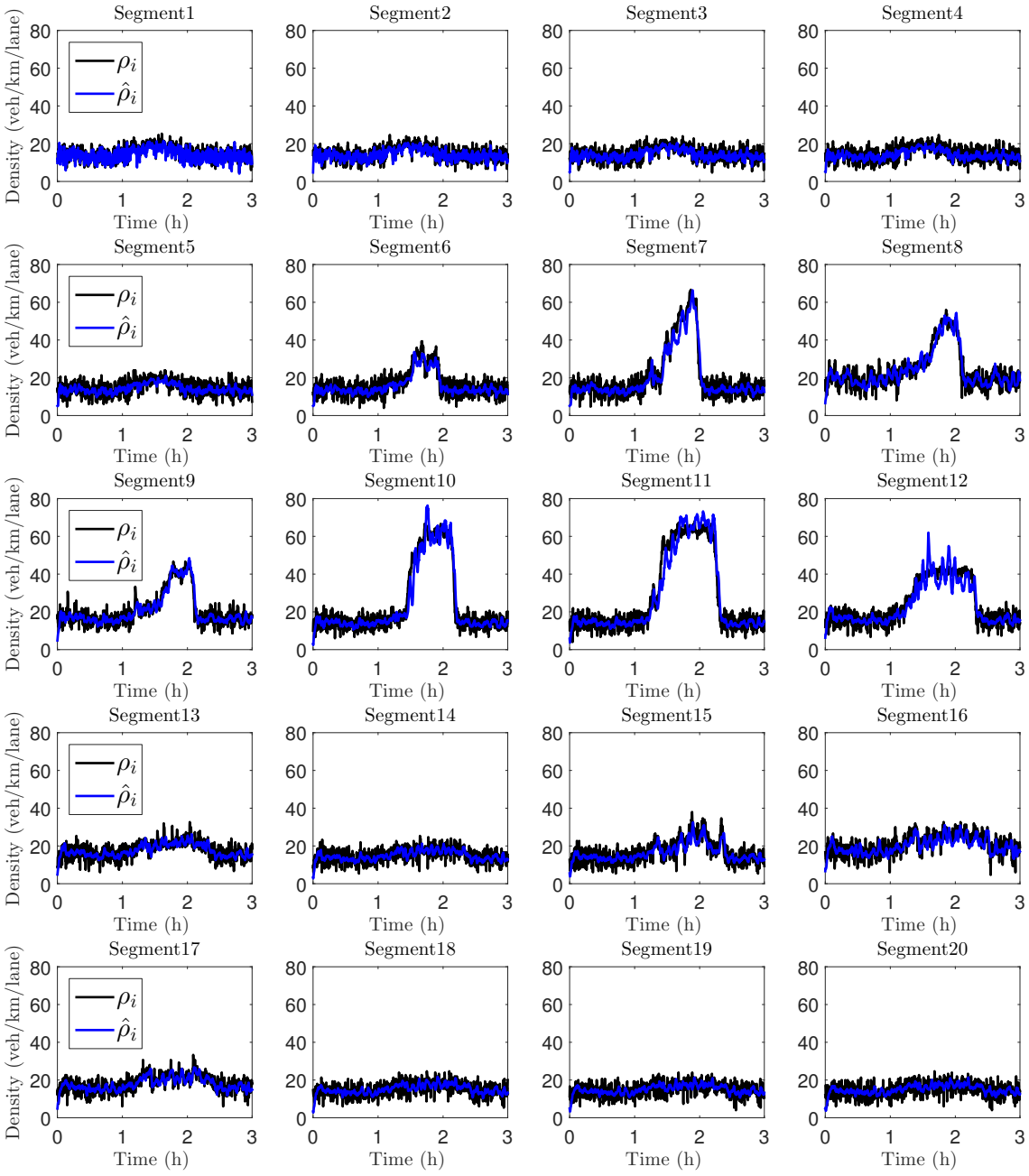


Fig. 7.10: Comparison between real (black line) and estimated (blue line) densities in veh/km/lane for all network segments for mixed traffic with a 20% penetration rate of ACC-equipped vehicles when the speed fed to the filter is calculated via (6.1) with $n = 12$.

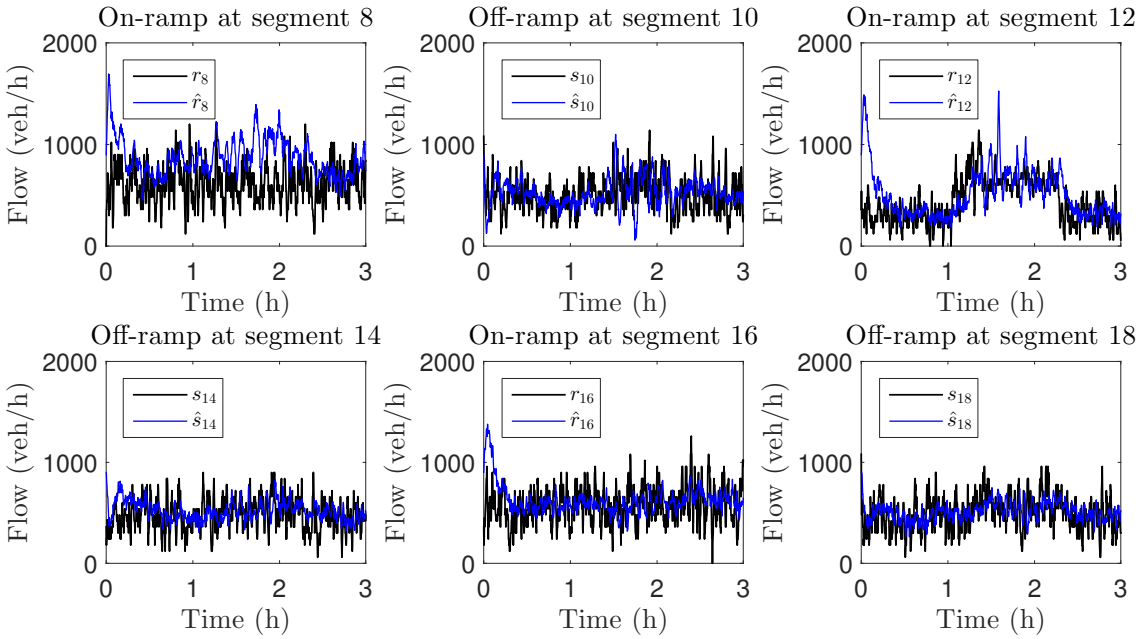


Fig. 7.11: Comparison between real (black line) and estimated (blue line) ramp flows in veh/h for all network ramps for mixed traffic with a 20% penetration rate of ACC-equipped vehicles when the speed fed to the filter is calculated via (6.1) with $n = 12$.

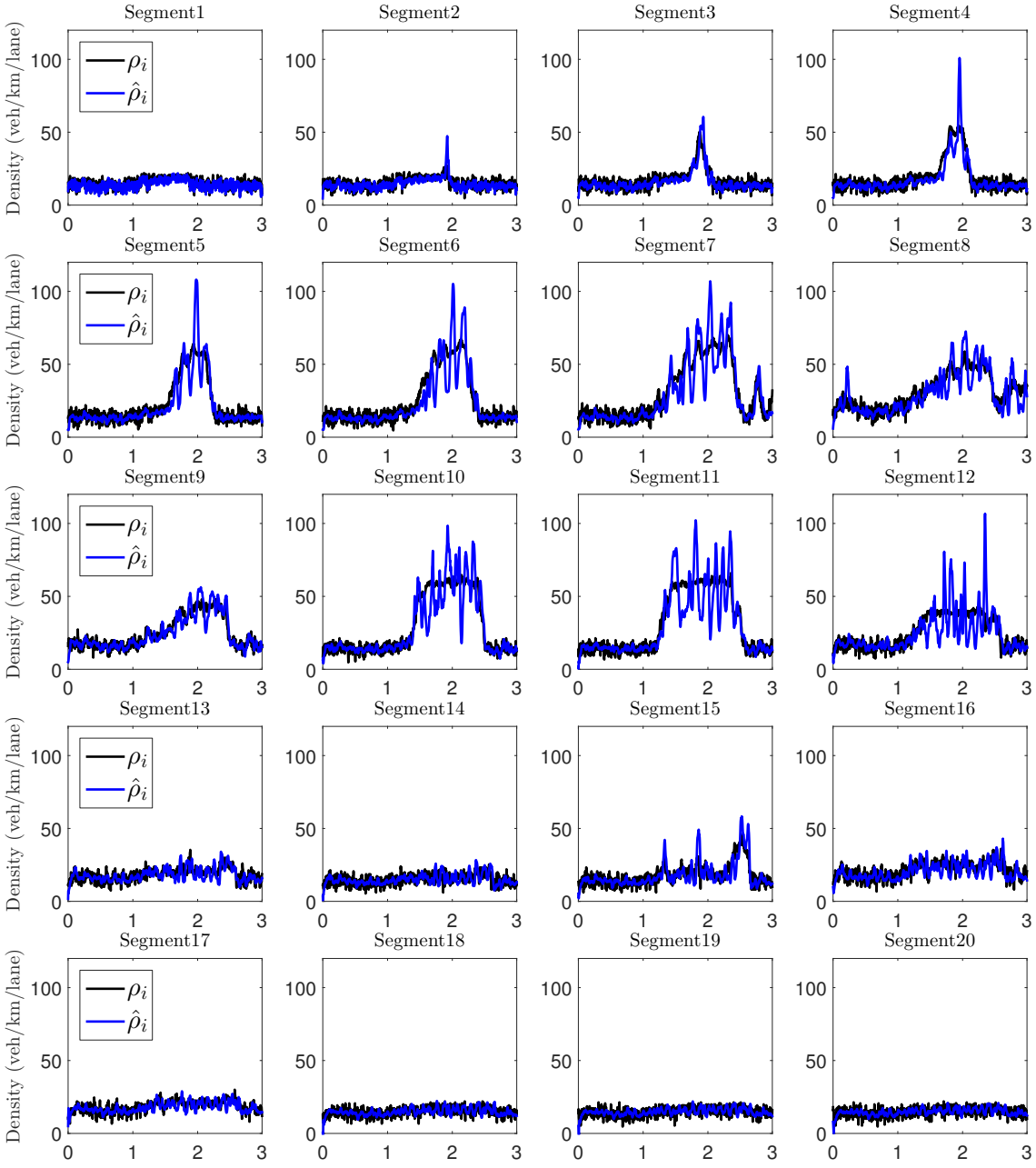


Fig. 7.12: Comparison between real (black line) and estimated (blue line) density per lane in veh/km for all network segments for mixed traffic with a 5% penetration rate of ACC-equipped vehicles when the speed fed to the filter is calculated via (6.1) with $n = 12$

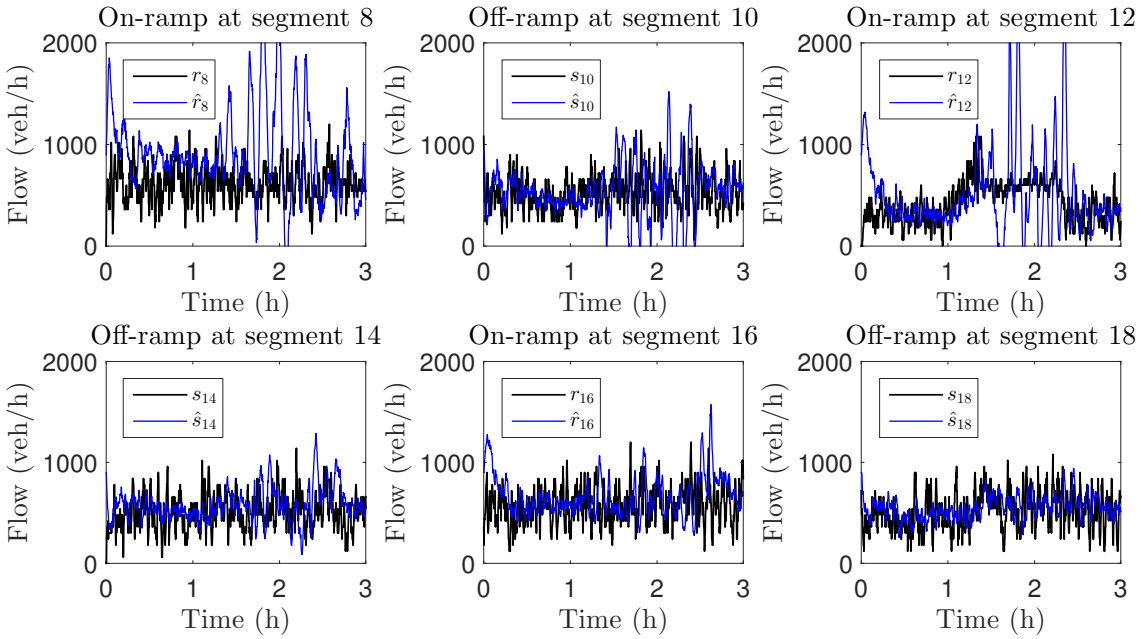


Fig. 7.13: Comparison between real (black line) and estimated (blue line) ramp flow in veh/h for all network on-ramps and off-ramps for mixed traffic with a 5% penetration rate of ACC-equipped vehicles when the speed fed to the filter is calculated via (6.1) with $n = 12$

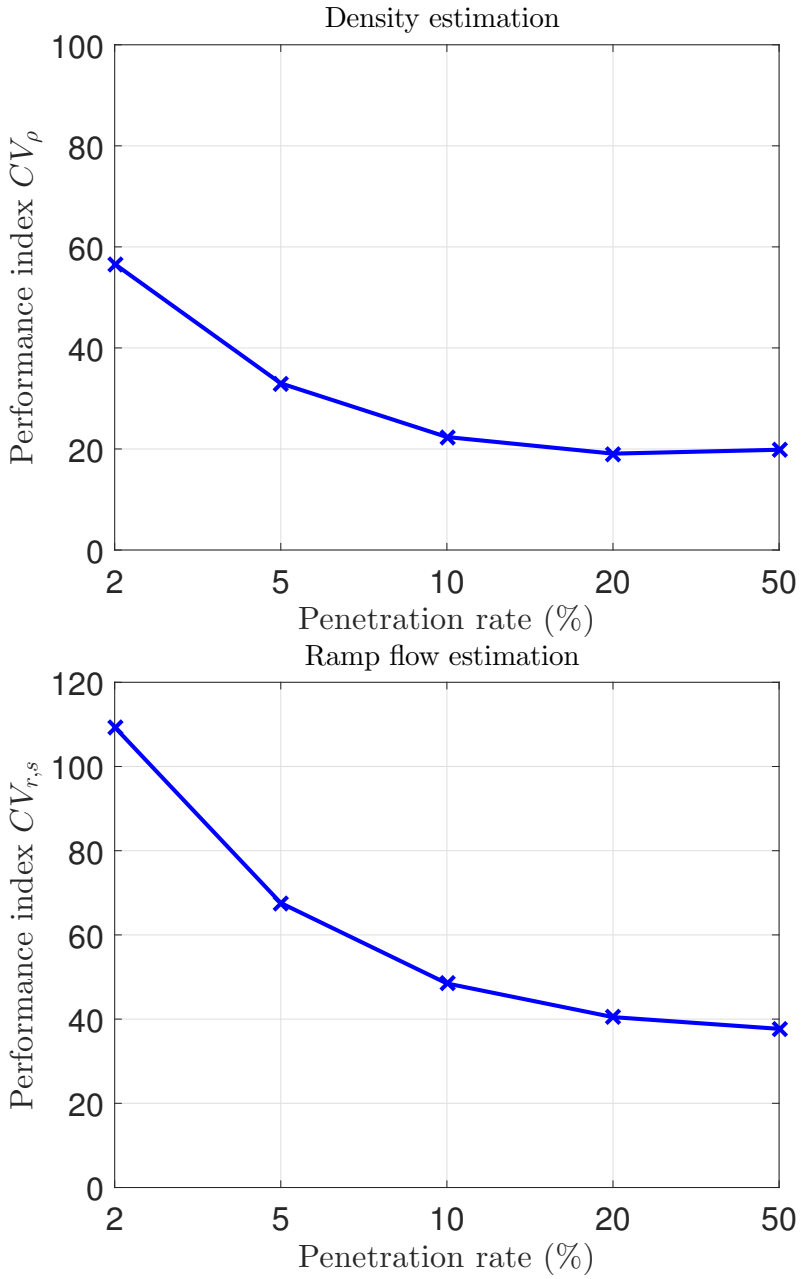


Fig. 7.14: Performance indices of density estimation $CV_\rho$ (top) calculated via (4.1) and ramp flow estimation $CV_{r,s}$ (bottom) calculated via (5.3) for varying penetration rates of ACC-equipped vehicles when the speed fed to the filter is calculated via (6.1) with $n = 12$.

.

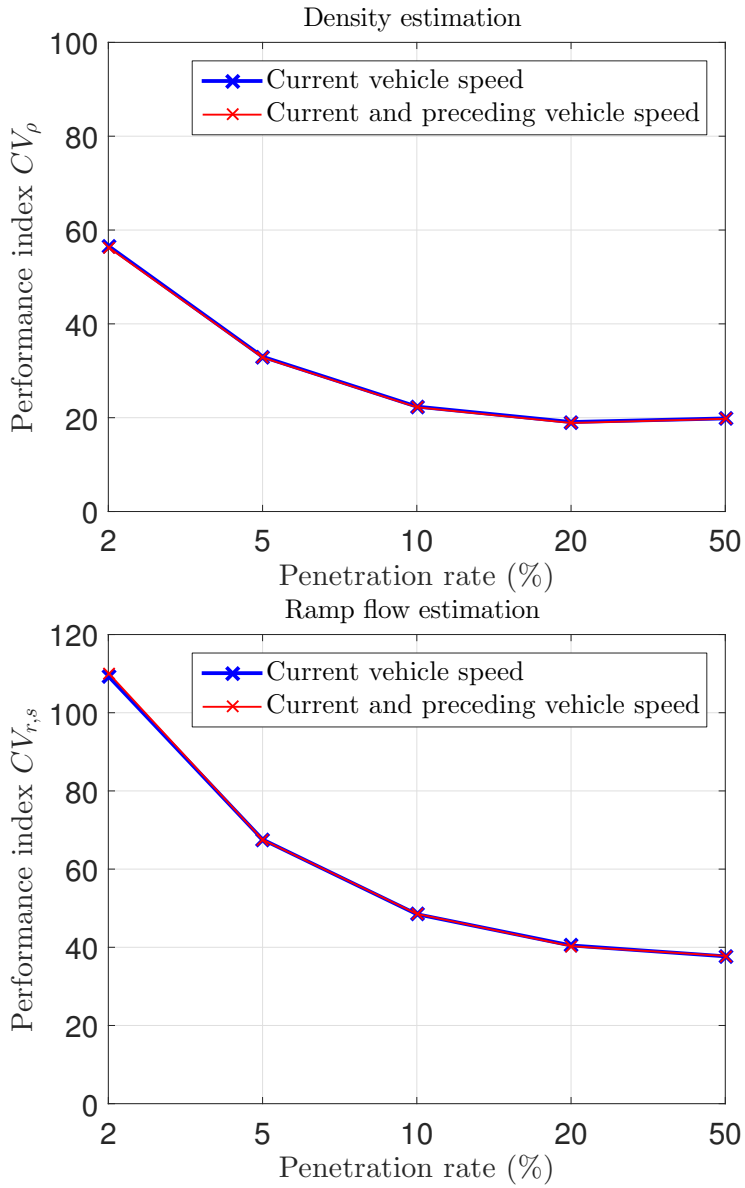


Fig. 7.15: Performance comparison between different speed reporting schemes of ACC-equipped vehicles for varying penetration rates. The performance indices of density estimation $CV_\rho$ (top) and of ramp flow estimation $CV_{r,s}$ (bottom) are calculated via (4.1) and (5.3), respectively, and the speed fed to the filter is calculated via (6.1) with $n = 12$.

# Chapter 8

# Conclusions

The estimation scheme proposed in Bekiaris-Liberis et al. (2016) has been thoroughly tested in a microscopic simulation platform using the traffic simulator Aimsun of TSS (Transport Simulation Systems, 2014). A highway stretch that contains on-ramps and off-ramps and features a dynamic inflow demand has been employed for testing the estimation performance in both congested and free-flow conditions for varying penetration rates of connected vehicles, in two different scenarios. In the first scenario, conventional and connected vehicles have statistically identical car-following behavior; whereas in the second scenario the connected vehicles are ACC-equipped and feature a different car-following behavior than conventional vehicles. In both cases the proposed scheme has proven effective in estimating segment densities and ramp flows for various penetration rates of connected vehicles. More specifically, in the case of conventionally-driven connected vehicles, density estimation is very satisfactory for penetration rates as low as 2%, while ramp flow estimation is very satisfactory for penetration rates of 5% or higher, but fair even at lower penetrations. In the case of ACC-equipped connected vehicles with strongly different longitudinal behavior compared to conventional vehicles, density estimation is very satisfactory for penetration rates of 5% or higher, but fair even at lower penetrations; while ramp flow is very satisfactory for penetration rates of 10% or higher, but fair even at lower penetrations. Moreover, an additional scenario, where ACC-equipped vehicles can also report the speed of the preceding vehicle, has been tested. The results have shown that this addition does not improve the estimation performance. Finally, the estimation performance has been proven to be quite insensitive to the choice of the filter parameters, which indicates that no serious fine-tuning effort will be required in field applications.

# Bibliography


Abou-Jaoude, R. (2003). ACC radar sensor technology, test requirements, and test solutions. *IEEE Transactions on Intelligent Transportation Systems 4*(3), 115–122.

Alvarez-Icaza, L., L. Munoz, X. Sun, and R. Horowitz (2004). Adaptive observer for traffic density estimation. In *IEEE American Control Conference*, Volume 3, pp. 2705 – 2710.

Bar-Gera, H. (2007). Evaluation of a cellular phone-based system for measurements of traffic speeds and travel times: A case study from Israel. *Transportation Research Part C: Emerging Technologies 15*(15), 380–391.

Bekiaris-Liberis, N., C. Roncoli, and M. Papageorgiou (2016). Highway traffic state estimation with mixed connected and conventional vehicles using speed measurements. *IEEE Transactions on Intelligent Transportation Systems,* to appear, DOI: 10.1109/TITS.2016.2552639.

Bishop, R. (2005). *Intelligent vehicle technology and trends*. Norwood MA, USA: Artech House Publishers.

Bose, A. and P. Ioannou (2003). Mixed manual/semi-automated traffic: a macroscopic analysis. *Transportation Research Part C: Emerging Technologies 11*(6), 439 – 462.

Darbha, S. and K. Rajagopal (1999). Intelligent cruise control systems and traffic flow stability. *Transportation Research Part C: Emerging Technologies 7*(6), 329 – 352.

Dargay, J., D. Gately, and M. Sommer (2007). Vehicle ownership and income growth, worldwide: 1960-2030. *The Energy Journal 28*(4), 143–170.

De Fabritiis, C., R. Ragona, and G. Valenti (2008). Traffic estimation and prediction based on real time floating car data. In *IEEE Conference on Intelligent Transportation Systems*, pp. 197–203.

Diakaki, C., M. Papageorgiou, I. Papamichail, and I. Nikolos (2015). Overview and analysis of Vehicle Automation and Communication Systems from a motorway traffic management perspective . *Transportation Research Part A: Policy and Practice 75*, 147 – 165.

Dragutinovic, N., K. A. Brookhuis, M. P. Hagenzieker, and V. A. Marchau (2005). Behavioural effects of advanced cruise control use: A meta-analytic approach. *European Journal of Transport and Infrastructure Research 5*(4), 267–280.

Garber, N. J. and R. Gadirau (1989). Factors affecting speed variance and its influence on accidents. *Transportation Research Record: Journal of the Transportation Research Board 1213*, 64–71.

Gayah, V. and V. Dixit (2013). Using mobile probe data and the macroscopic fundamental diagram to estimate network densities: Tests using microsimulation. *Transportation Research Record: Journal of the Transportation Research Board 2390*, 76–86.

Ge, J. I. and G. Orosz (2014). Dynamics of connected vehicle systems with delayed acceleration feedback. *Transportation Research Part C: Emerging Technologies 46*, 46 – 64.

Gipps, P. G. (1981). A behavioural car-following model for computer simulation. *Transportation Research Part B: Methodological 15*(2), 105–111.

Gipps, P. G. (1986). A model for the structure of lane-changing decisions. *Transportation Research Part B: Methodological 20*(5), 403–414.

Hegyi, A., D. Girimonte, R. Babuška, and B. De Schutter (2006). A comparison of filter configurations for freeway traffic state estimation. In *IEEE Conference on Intelligent Transportation Systems*, pp. 1029–1034.

Herrera, J. C., D. B. Work, R. Herring, X. J. Ban, Q. Jacobson, and A. M. Bayen (2010). Evaluation of traffic data obtained via GPS-enabled mobile phones: The Mobile Century field experiment. *Transportation Research Part C: Emerging Technologies 18*(4), 568 – 583.

Kesting, A., M. Treiber, M. Schnhof, and D. Helbing (2007). Extending adaptive cruise control to adaptive driving strategies. *Transportation Research Record: Journal of the Transportation Research Board 2000*, 16–24.

Kesting, A., M. Treiber, M. Schönhof, and D. Helbing (2008). Adaptive cruise control design for active congestion avoidance. *Transportation Research Part C: Emerging Technologies 16*(6), 668–683.

Liang, C.-Y. and H. Peng (1999). Optimal adaptive cruise control with guaranteed string stability. *Vehicle System Dynamics 32*(4-5), 313–330.

Lovisari, E., C. C. de Wit, and A. Kibangou (2015). Flow and density reconstruction and optimal sensor placement for road transportation networks. Under review, available at arXiv: 1507.07093.

Marsden, G., M. McDonald, and M. Brackstone (2001). Towards an understanding of adaptive cruise control. *Transportation Research Part C: Emerging Technologies 9*(1), 33 – 51.

Messelodi, S., C. M. Modena, M. Zanin, F. G. D. Natale, F. Granelli, E. Betterle, and A. Guarise (2009). Intelligent extended floating car data collection. *Expert Systems with Applications 36*(3, Part 1), 4213 – 4227.

Mihaylova, L., R. Boel, and A. Hegyi (2007). Freeway traffic estimation within particle filtering framework. *Automatica 43*(2), 290 – 300.

Morbidi, F., L. L. Ojeda, C. C. De Wit, and I. Bellicot (2014). A new robust approach for highway traffic density estimation. In *European Control Conference*, pp. 2575–2580.

Muñoz, L., X. Sun, R. Horowitz, and L. Alvarez (2003). Traffic density estimation with the cell transmission model. In *American Control Conference*, pp. 3750–3755.

Ntousakis, I. A., I. K. Nikolos, and M. Papageorgiou (2015). On microscopic modelling of adaptive cruise control systems. In *Transportation Research Procedia*, pp. 111–127.

Papageorgiou, M., M. Ben-Akiva, J. Bottom, P. Bovy, S. Hoogendoorn, N. Hounsell, A. Kotsialos, and M. McDonald (2007). ITS and traffic management. In C. Barnhart and G. Laporte (Eds.), *Transportation*, Volume 14 of *Handbooks in Operations Research and Management Science*, Chapter 11, pp. 715 – 774.

Piccoli, B., K. Han, T. L. Friesz, T. Yao, and J. Tang (2015). Second-order models and traffic data from mobile sensors. *Transportation Research Part C: Emerging Technologies 52*, 32 – 56.

Rahmani, M., H. N. Koutsopoulos, and A. Ranganathan (2010). Requirements and potential of GPS-based floating car data for traffic management: Stockholm case study. In *IEEE Conference on Intelligent Transportation Systems*, pp. 730–735.

Rajamani, R., D. Levinson, P. Michalopoulos, J. Wang, K. Santhanakrishnan, and X. Zou (2005). Adaptive cruise control system design and its impact on traffic flow. Project Report CTS 05-01, University of Minnesota, Department of Civil Engineering.

Rajamani, R. and S. Shladover (2001). An experimental comparative study of autonomous and co-operative vehicle-follower control systems. *Transportation Research Part C: Emerging Technologies 9*(1), 15 – 31.

Ramezani, M. and N. Geroliminis (2012). On the estimation of arterial route travel time distribution with Markov chains. *Transportation Research Part B 46*(10), 1576 – 1590.

Rao, B. and P. Varaiya (1994). Roadside intelligence for flow control in an intelligent vehicle and highway system. *Transportation Research Part C: Emerging Technologies 2*(1), 49 – 72.

Rempe, F. and K. Bogenberger (2016). A comparison of traffic estimation algorithms based on floating car data. Presented at *1st Symposium on Management of Future motorway and urban Traffic Systems, Chania, Greece*.

Roncoli, C., N. Bekiaris-Liberis, and M. Papageorgiou (2016). Highway traffic state estimation using speed measurements: case studies on NGSIM data and highway A20 in the Netherlands. *Transportation Research Record,* to appear.

Roncoli, C., M. Papageorgiou, and I. Papamichail (2015). Traffic flow optimisation in presence of vehicle automation and communication systems Part II: Optimal control for multi-lane motorways. *Transportation Research Part C: Emerging Technologies 57*, 260 – 275.

Roncoli, C., I. Papamichail, and M. Papageorgiou (2016). Hierarchical model predictive control for multi-lane motorways in presence of Vehicle Automation and Communication Systems. *Transportation Research Part C: Emerging Technologies 62*, 117–132.

Seo, T., T. Kusakabe, and Y. Asakura (2015). Estimation of flow and density using probe vehicles with spacing measurement equipment. *Transportation Research Part C: Emerging Technologies 53*, 134 – 150.

Shladover, S., D. Su, and X.-Y. Lu (2012). Impacts of cooperative adaptive cruise control on freeway traffic flow. *Transportation Research Record: Journal of the Transportation Research Board 2324*, 63–70.

Transport Simulation Systems (2014). *Aimsun 8 Dynamic Simulators Users' Manual*. Transport Simulation Systems.

Treiber, M. and D. Helbing (2001). Microsimulations of freeway traffic including control measures. *Automatisierungstechnik Methoden und Anwendungen der Steuerungs, Regelungs und Informationstechnik 49*(11), 478.

Treiber, M. and A. Kesting (2013). *Traffic flow dynamics*. New York: Springer.

Treiber, M., A. Kesting, and R. E. Wilson (2011). Reconstructing the traffic state by fusion of heterogeneous data. *Computer-Aided Civil and Infrastructure Engineering 26*(6), 408–419.

Turksma, S. (2000). The various uses of floating car data . In *Conference on Road Transport Information and Control*, pp. 51–55.

van Arem, B., C. J. van Driel, and R. Visser (2006). The impact of cooperative adaptive cruise control on traffic-flow characteristics. *IEEE Transactions on Intelligent Transportation Systems 7*(4), 429–436.

VanderWerf, J., S. Shladover, N. Kourjanskaia, M. Miller, and H. Krishnan (2001). Modeling effects of driver control assistance systems on traffic. *Transportation Research Record: Journal of the Transportation Research Board 1748*, 167–174.

Varaiya, P. (1993). Smart cars on smart roads: problems of control. *IEEE Transactions on Automatic Control 38*(2), 195–207.

Wang, M., W. Daamen, S. P. Hoogendoorn, and B. van Arem (2014). Rolling horizon control framework for driver assistance systems. Part II: Cooperative sensing and cooperative control . *Transportation Research Part C: Emerging Technologies 40*, 290 – 311.

Wang, Y. and M. Papageorgiou (2005). Real-time freeway traffic state estimation based on extended Kalman filter: a general approach. *Transportation Research Part B: Methodological 39*(2), 141 – 167.

Waterson, B. and S. Box (2012). Quantifying the impact of probe vehicle localisation data errors on signalised junction control. *Intelligent Transport Systems 6*(2), 197–203.

Work, D. B., O.-P. Tossavainen, S. Blandin, A. M. Bayen, T. Iwuchukwu, and K. Tracton (2008). An ensemble Kalman filtering approach to highway traffic estimation using GPS enabled mobile devices. In *IEEE Conference on Decision and Control*, pp. 5062–5068.

Yim, Y. and R. Cayford (2001). Investigation of vehicles as probes using global positioning system and cellular phone tracking: field operational test. *California Partners for Advanced Transit and Highways*.

Yuan, Y., J. Van Lint, R. E. Wilson, V. Wageningen-Kessels, S. P. Hoogendoorn, et al. (2012). Real-time lagrangian traffic state estimator for freeways. *IEEE Transactions on Intelligent Transportation Systems 13*(1), 59–70.

Yue, Y. (2009). A traffic-flow parameters evaluation approach based on urban road video. *International Journal of Intelligent Engineering & Systems 2*(1), 33–39.

Zhang, C., X. Yang, and X. Yan (2007). Methods for floating car sampling period optimization. *Journal of Transportation Systems Engineering and Information Technology 7*(3), 100 – 104.

Zhao, W., A. Goodchild, and E. McCormack (2011). Evaluating the accuracy of spot speed data from global positioning systems for estimating truck travel speed. *Transportation Research Record: Journal of the Transportation Research Board 2246*, 101–110.

Zito, R., G. D'Este, and M. Taylor (1995). Global positioning systems in the time domain: How useful a tool for intelligent vehicle-highway systems? *Transportation Research Part C: Emerging Technologies 3*(4), 193 – 209.